MAVS associates with the mitochondrial outer membrane guanosine triphosphatase, Mfn2

We next attempted to determine whether MAVS associated with previously unidentified cellular components by analyzing immunoprecipitated samples derived from HEK 293 cells stably expressing Myc-tagged MAVS. Analysis of samples immunoprecipitated with an antibody against the Myc tag by liquid chromatography with tandem mass spectrometry (LC/MS/MS) identified several mitochondrial proteins (table S1). Plasmids encoding these proteins were individually coexpressed with a plasmid encoding MAVS by transient transfection of HEK 293 cells. Of these candidates, the mitochondrial outer membrane guanosine triphosphatase (GTPase) Mfn2, which mediates mitochondrial fusion (*20*), coimmunoprecipitated with MAVS (Fig. 1B). In addition, we confirmed that MAVS coimmunoprecipitated with endogenous Mfn2 in HEK 293 cells (Fig. 1C). The interaction between endogenous Mfn2 and MAVS was also observed in mouse embryonic fibroblasts (MEFs) (fig. S1). Consistent with this observation, MAVS and Mfn2 mRNAs showed similar expression patterns in human tissues (*15*, *21*), and the colocalization of both endogenous proteins to mitochondria was confirmed in MEFs by fluorescence microscopy (Fig. 1D). Although Mfn2 is a large transmembrane GTPase that is well known for mediating mitochondrial fusion, it has additionally been reported to act as an endoplasmic reticulum (ER)–mitochondrion tether (*22*), as a suppressor of cellular proliferation (*23*) and as a pathogenic factor in inherited peripheral neuropathy (*24*).

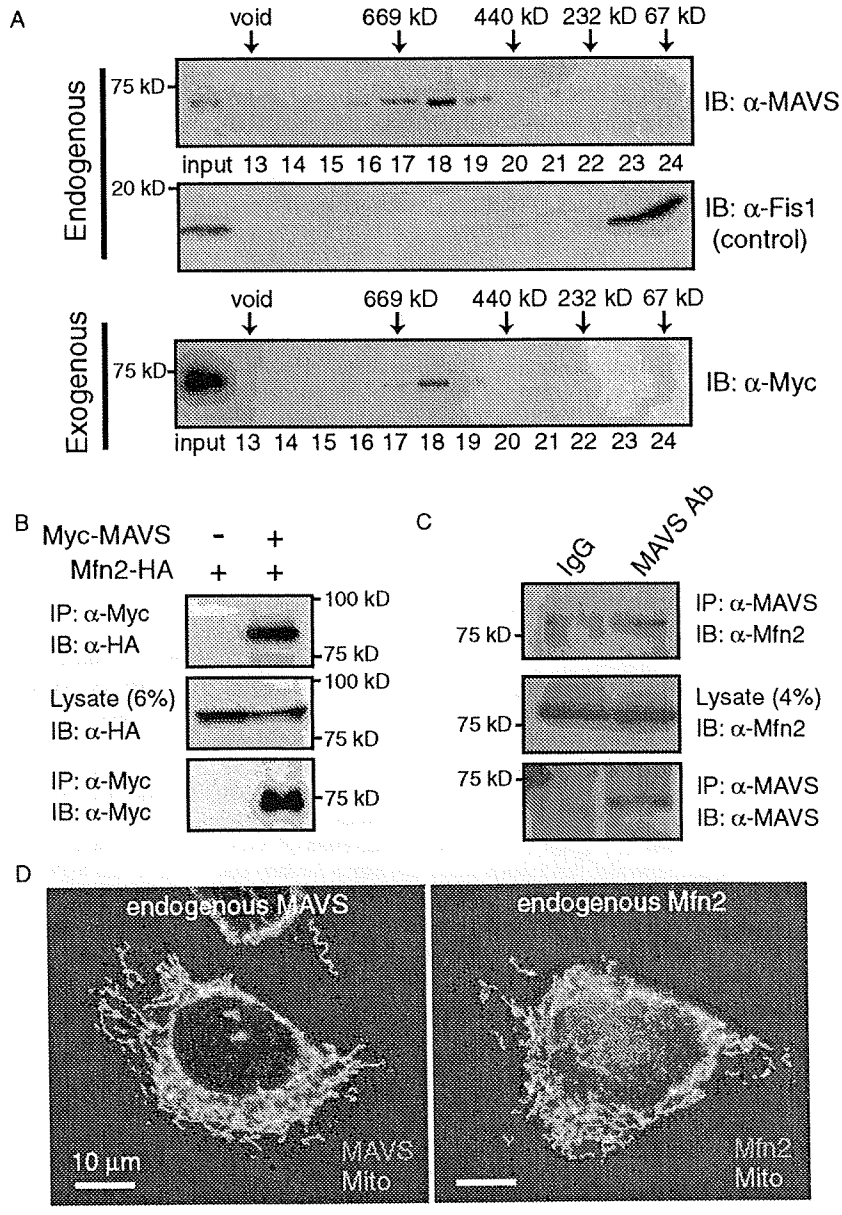

Fig. 1. MAVS is a component of a supramolecular protein complex. (A) Size exclusion chromatography (Superdex-200 HR-10/30 column) of endogenous and exogenous MAVS at pH 7.2. The positions corresponding to the elution of standard markers of molecular mass and the void volume are indicated. Fractions (numbered) were analyzed by Western blotting with a polyclonal antibody against hMAVS (to detect endogenous protein) or the 9E10 monoclonal antibody against Myc (to detect tagged protein), as well as with a polyclonal antibody against Fis1 for the control analysis. (B) HEK 293 cells were cotransfected with combinations of plasmids encoding HA-tagged Mfn2 and Myc-tagged MAVS, as indicated. Western blots of samples immunoprecipitated (IP) with an antibody against Myc or postnuclear cell lysates (lysate; 6% of the input) were analyzed by immunoblotting (IB) with either the monoclonal antibody HA.11 against HA or the monoclonal antibody 9E10 against Myc. (C) Interaction of endogenous Mfn2 with MAVS. Lysates of HEK 293 cells were subjected to immunoprecipitation with anti-MAVS polyclonal antibody or control IgG followed by the analysis of Western blots with an antibody against Mfn2. Lysate, 4% of the input. In (A) to (C), α denotes "anti-". (D) Endogenous MAVS (red) and Mfn2 (red) colocalize with mitochondria in MEFs. Mitochondria were stained with a monoclonal antibody against mtHsp70 (green). Scale bar, 10 μm.

Mfn2 inhibits MAVS-mediated activation of IRF-3 and NF-κB

Having identified Mfn2 as a component of the MAVS complex, we investigated whether this protein modulated MAVS-mediated activation of IFN-β and NF-κB reporter constructs. Although MAVS potently activated both IFN-β and NF-κB luciferase–based reporters, as seen previously (*9*, *14–16*), Mfn2 alone failed to activate either reporter construct (Fig. 2A). However, coexpression of Mfn2, but not the unrelated mitochondrial outer membrane protein Fis1, with MAVS was sufficient to inhibit MAVS-dependent activation of IFN-β and NF-κB reporters in a dose-dependent manner (Fig. 2B). This inhibitory activity was not observed with the Mfn2 homolog, Mfn1, despite the ~60% sequence identity between the two proteins (*21*), which indicated that the observed inhibitory activity toward MAVS-mediated signaling was specific to Mfn2 (Fig. 2C). The inhibition that resulted from the increased abundance of Mfn2 was not attributable to general mitochondrial dysfunction because most cells that contained both overexpressed MAVS and Mfn2 exhibited normal tubular mitochondrial morphology that was indistinguishable from that of untransfected cells (Fig. 2D).

Because MAVS-dependent antiviral signaling is potentiated by the recognition of viral dsRNA by the cytoplasmic RNA helicases RIG-I and MDA-5, we sought to determine the effect of Mfn2 on the ability of these sensor helicases and dsRNA to induce downstream activation of IRF-3 and the IFN-β reporter. Overexpression of the N-terminal CARD domains of RIG-I [designated as RIG-I(1–250) in this study] induces a robust intracellular antiviral response (*25*). Mfn2 dramatically reduced the ability of RIG-I(1–250) to activate the IFN-β reporter in a dose-dependent manner (Fig. 3A) and similarly reduced the production of endogenous IFN-β protein

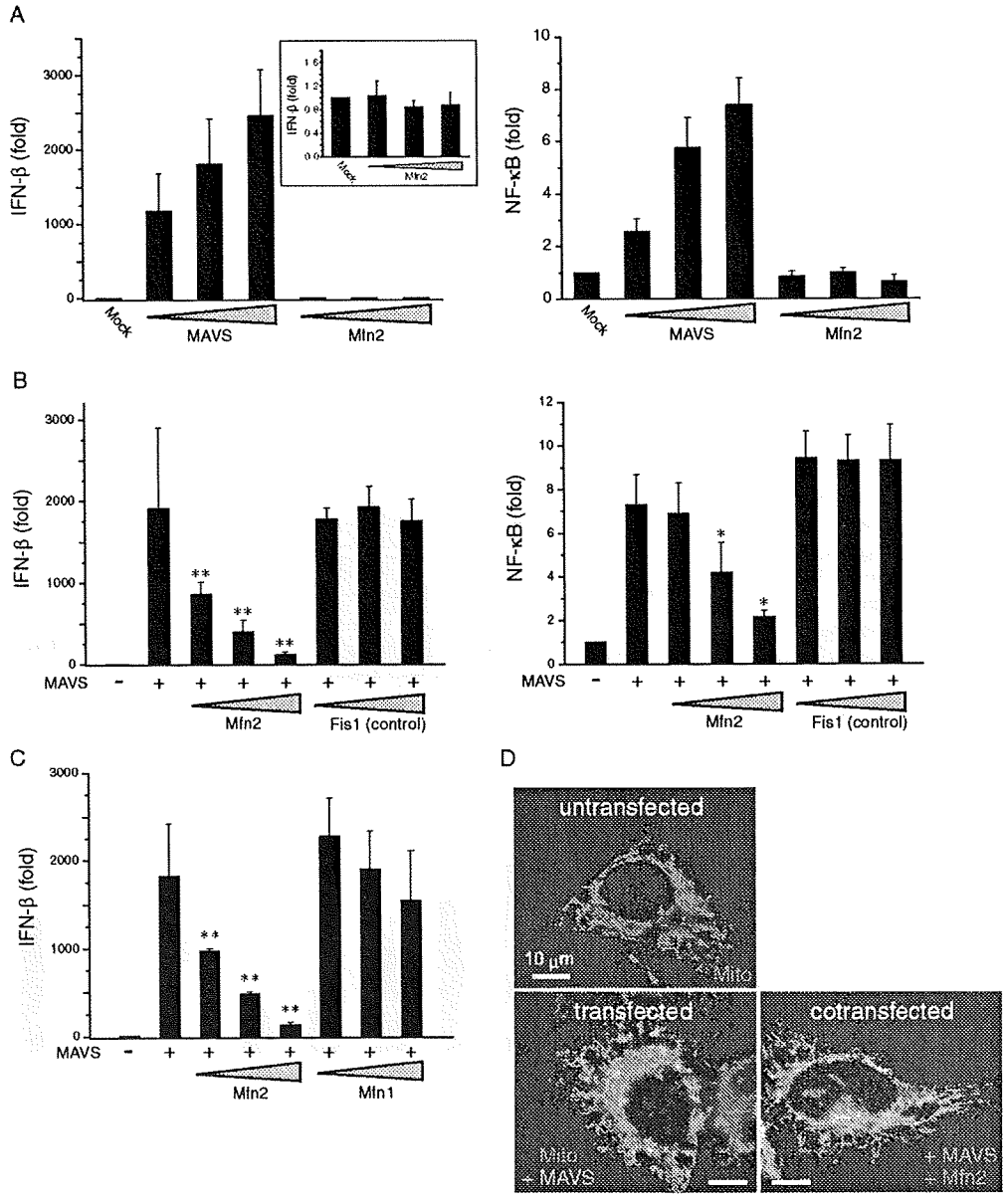

Fig. 2. Mfn2 inhibits MAVS-mediated activation of IFN-β and NF-κB reporters. (A) HEK 293 cells were transfected with empty vector (Mock) or increasing amounts (20, 50, and 100 ng) of plasmids encoding MAVS (positive control) or Mfn2 and with either IFN-β (left panel) or NF-κB (right panel) luciferase reporter plasmids. Inset: a magnified scale of Mfn2 result. (B) HEK 293 cells were cotransfected with 50 ng of a plasmid encoding MAVS and increasing amounts (20, 50, and 100 ng) of plasmids encoding Mfn2 or Fis1 (negative control) together with the same reporter plasmids used in (A). (C) The Mfn2 homolog, Mfn1, does not inhibit MAVS-mediated activation of IFN-β reporter. The resulting IFN-β reporter activity was determined as above. All data shown represent mean values ± SD (n = 3 experiments). *P < 0.05; **P < 0.01. (D) Immunofluorescence microscopy of untransfected HeLa cells, HeLa cells transfected with a plasmid encoding MAVS, or HeLa cells cotransfected with plasmids encoding MAVS and Mfn2. Cells were visualized with MAVS [enhanced green fluorescent protein; green], Mfn2 (Alex Fluor 568; red), and mitochondria (red fluorescent protein; red). Scale bar, 10 μm.

as determined by enzyme-linked immunosorbent assay (ELISA) (Fig. 3B). We additionally examined the activation of endogenous IRF-3 by performing gel-shift assays. Expression of RIG-I(1–250) promoted the hallmarks of IRF-3 activation, namely, its dimerization and phosphorylation (Fig. 3C), both of which were impaired by Mfn2 in a dose-dependent manner (Fig. 3C).

Overexpression of Mfn2 additionally abrogated the effect of MDA-5 in a dose-dependent manner (Fig. 3D). MDA-5 is the intracellular receptor for poly(I:C), a synthetic analog of viral double-stranded RNA (*26*, *27*). Consistent with previous findings, the delivery of poly(I:C) into HEK 293 cells by transient transfection stimulated the IFN-β response, which was suppressed by Mfn2 (Fig. 3E). In contrast, Mfn2 did not impair the IFN-β response to extracellular poly(I:C) (Fig. 3E). Taken together, these results indicate that Mfn2 acted as a negative regulator of RIG-I–, MDA-5–, and dsRNA-dependent antiviral signaling through MAVS and suggested that the association of MAVS and Mfn2 might underlie this inhibition.

Loss of endogenous Mfn2 results in enhanced RIG-I– and MDA-5–induced antiviral responses

The previous experiments showed that Mfn2 suppressed MAVS-dependent signaling. We therefore attempted to determine, through an RNA interference

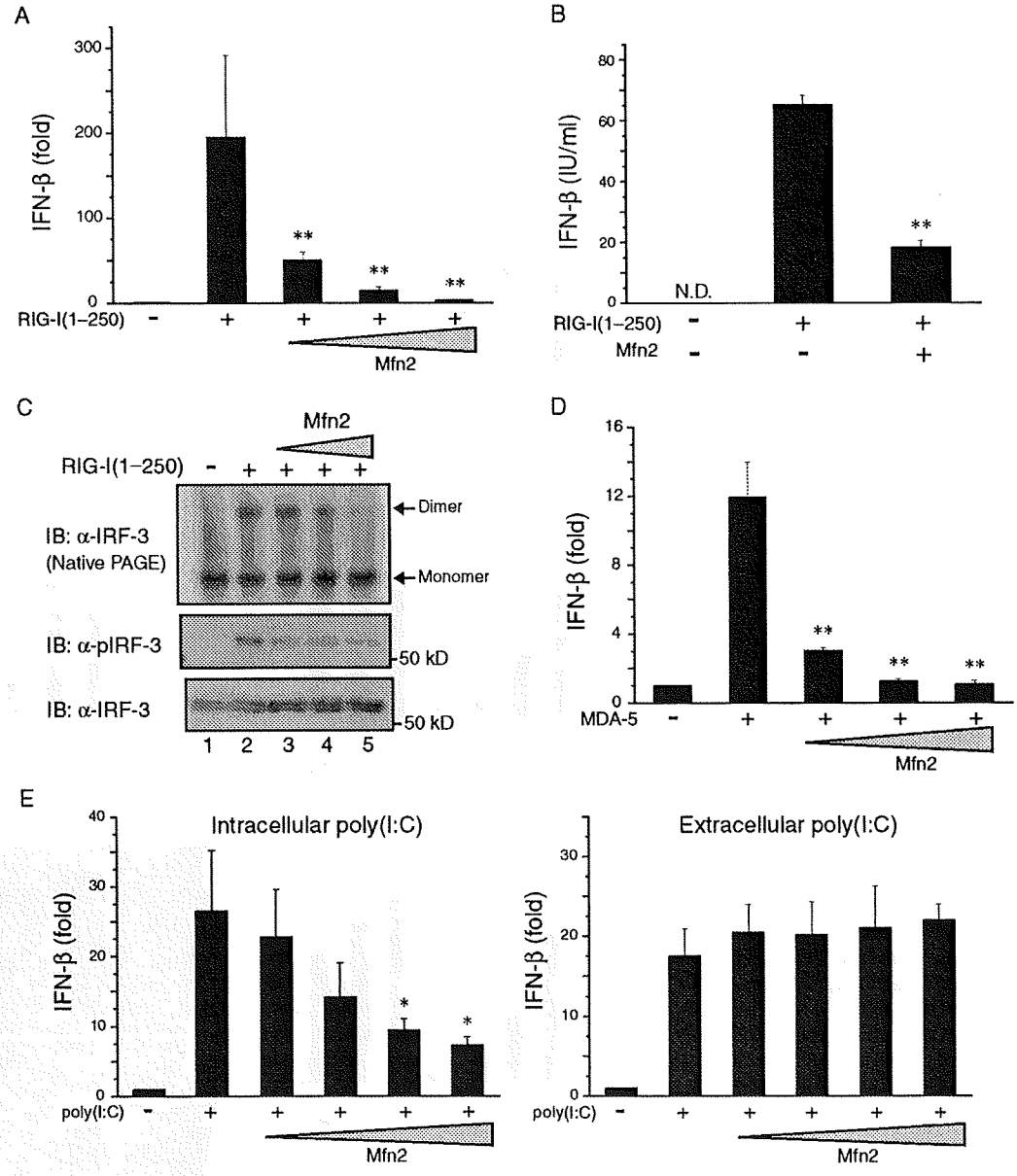

Fig. 3. Mfn2 suppresses IFN-β signaling mediated by RIG-I and MDA-5. (A) HEK 293 cells were cotransfected with 50 ng of plasmid encoding RIG-I(1–250) with increasing amounts (20, 50, and 100 ng) of a plasmid encoding Mfn2 together with the luciferase reporter plasmid p125luc. Transfected cells were analyzed 24 hours later for IFN-β–dependent luciferase activity. (B) HEK 293 cells were cotransfected with 200 ng of plasmid encoding RIG-I(1–250) and 200 ng of a plasmid encoding either pcDNA3.1 (negative) or Mfn2. Culture supernatants were harvested 24 hours after transfection and analyzed by ELISA to measure the production of IFN-β. (C) HEK 293 cells were cotransfected with 300 ng of a plasmid encoding RIG-I(1–250) and increasing amounts (100, 300, and 500 ng) of the plasmid encoding Mfn2. Cell lysates were resolved by electrophoresis under native (top panel) or denaturing conditions (middle and bottom panels) and then analyzed by Western blotting with the indicated antibodies. (D) Experiments were performed similarly to those in (A), except that the plasmid encoding MDA-5 was used in the transfections instead of the plasmid encoding RIG-I(1–250). (E) HEK 293 cells were transfected with various amounts (20, 50, 100, and 200 ng) of the plasmid encoding Mfn2 and were either cotransfected with poly(I:C) (left panel) or treated extracellularly with poly(I:C) (right panel). The resulting IFN-β reporter activity was determined as described earlier. All data shown represent mean values ± SD (n = 3 experiments). *$P < 0.05$; **$P < 0.01$.

approach, whether endogenous Mfn2 was responsible for modulating the MAVS-dependent transcriptional activation of the gene encoding IFN-β. Consistent with our previous findings, HEK 293 cells that had been treated with Mfn2-specific small interfering RNA (siRNA), which efficiently knocked down the amount of endogenous Mfn2 protein by greater than 90% (Fig. 4, A and B), exhibited enhanced induction of the IFN-β reporter construct in response to RIG-I(1–250) relative to that of control siRNA–transfected cells (Fig. 4B). Moreover, reintroduction of Myc-tagged Mfn2 into HEK 293 cells that had been treated with Mfn2-specific siRNA restored the suppressive effect on RIG-I(1–250)–dependent induction of the IFN-β reporter (Fig. 4C). HEK 293 cells also exhibited a differential response to an increased abundance of MAVS when treated with the Mfn2-specific siRNA, with increased activation of the IFN-β reporter and production of endogenous IFN-β relative to that of cells treated with the control siRNA (fig. S2, A and B). Knockdown of endogenous Mfn2 by siRNA similarly enhanced the activation of the IFN-β reporter and the production of IFN-β

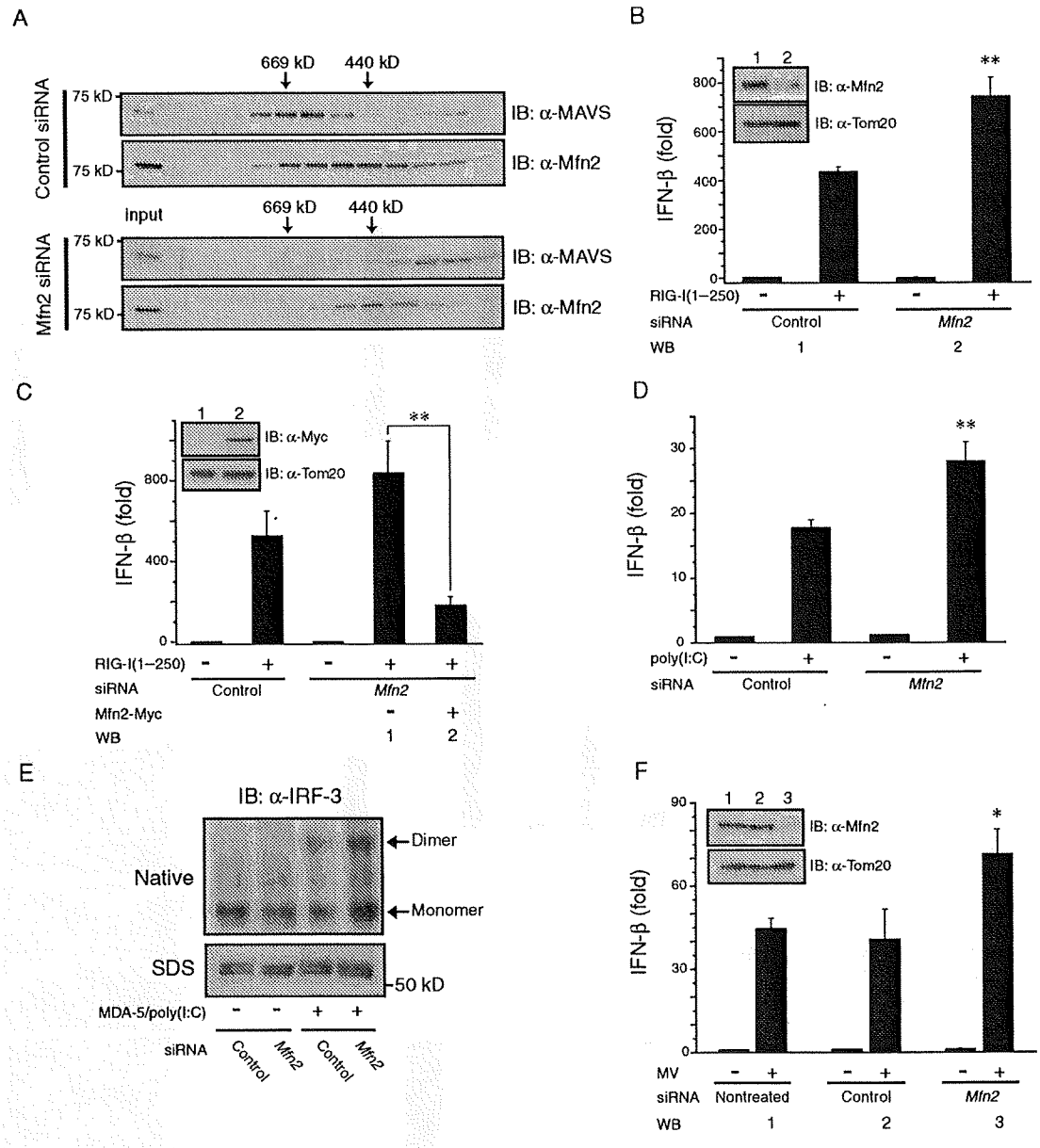

Fig. 4. Treatment with Mfn2-specific siRNA results in an enhanced antiviral response. (A) Gel filtration (Superose 6 HR-10/30) elution profiles of endogenous Mfn2 (as well as MAVS) extracted from the mitochondrial fraction of HEK 293 cells that had been treated with either control siRNA or siRNA specific for Mfn2. The positions corresponding to the elution of 669- and 440-kD molecular mass markers are indicated, and fractions were analyzed by Western blotting with antibodies against Mfn2 and MAVS. (B) HEK 293 cells were transfected with either control siRNA or siRNA specific for Mfn2 to evaluate the effect of knockdown of Mfn2 on the antiviral response. Twenty-four hours later, siRNA-treated cells were retransfected with the IFN-β reporter plasmid together with a plasmid encoding RIG-I(1–250). The efficiency of knockdown of Mfn2 (inset, lane 2) was confirmed by analysis of Western blots (WB) with a monoclonal antibody against Mfn2, and Tom20 was used as a loading control. (C) Experiments were performed similarly to those described in (B), except that IFN-β reporter-dependent luciferase activity was additionally measured after reintroduction of Myc-tagged Mfn2. Expression of the plasmid encoding Myc-tagged Mfn2 was confirmed by Western blotting analysis with an antibody (9E10) against Myc (inset, lane 2). (D) Experiments were performed similarly to those in (B), except that cells were transfected with poly(I:C) instead of the plasmid encoding RIG-I(1–250). (E) Knockdown of Mfn2 enhanced MDA-5–induced activation of IRF-3. (F) Activation of the IFN-β reporter in siRNA-treated HEK 293 cells infected with measles virus (MV) at an MOI of 2. All data shown represent mean values ± SD (n = 3 experiments). *P < 0.05; **P < 0.01.

protein in response to transfection with poly(I:C) (Fig. 4D and fig. S3), as well as increasing the amount of MDA-5–induced dimerized IRF-3 (Fig. 4E). Consistent with these findings, activation of the IFN-β reporter in response to infection with measles virus (MV), an RNA virus of the *Paramyxoviridae* family, was also enhanced in the cells treated with Mfn2-specific siRNA compared to that in control cells (Fig. 4F).

Given that our knockdown experiments failed to completely deplete Mfn2 protein (the effects were relatively modest), we evaluated IFN-β responses in wild-type (WT) and *Mfn2*-deficient MEFs (*28*). MAVS- and RIG-I–dependent production of IFN-β was significantly enhanced (>4-fold) in the *Mfn2*-deficient cells compared to that of WT cells (Fig. 5A). In addition, reintroduction of Myc-tagged murine Mfn2, but not that of its homolog mMfn1, fully restored suppression of IFN-β production in MEFs from $Mfn2^{-/-}$ mice (Fig. 5B), underscoring the importance of endogenous Mfn2 for the modulation of MAVS-mediated antiviral responses. When the $Mfn2^{-/-}$ MEFs were infected with a recombinant vesicular stomatitis virus (VSV) expressing green fluorescent protein (GFP) (VSVΔG*-G) (*29*), the production of IFN-β protein was substantially increased relative to that of infected WT and *Mfn1*-deficient MEFs (Fig. 5C), and the number of cells expressing GFP was significantly reduced only in the *Mfn2*-deficient MEFs, indicating their increased resistance to VSV infection (Fig. 5D). Furthermore, induction of IFN-β production by a positive-stranded RNA virus of the *Picornavirus* family, encephalomyocarditis virus (EMCV), was also greater in the *Mfn2*-deficient MEFs relative to that of WT MEFs (Fig. 5E), consistent with a role for Mfn2 as an inhibitor of the MAVS-mediated antiviral response.

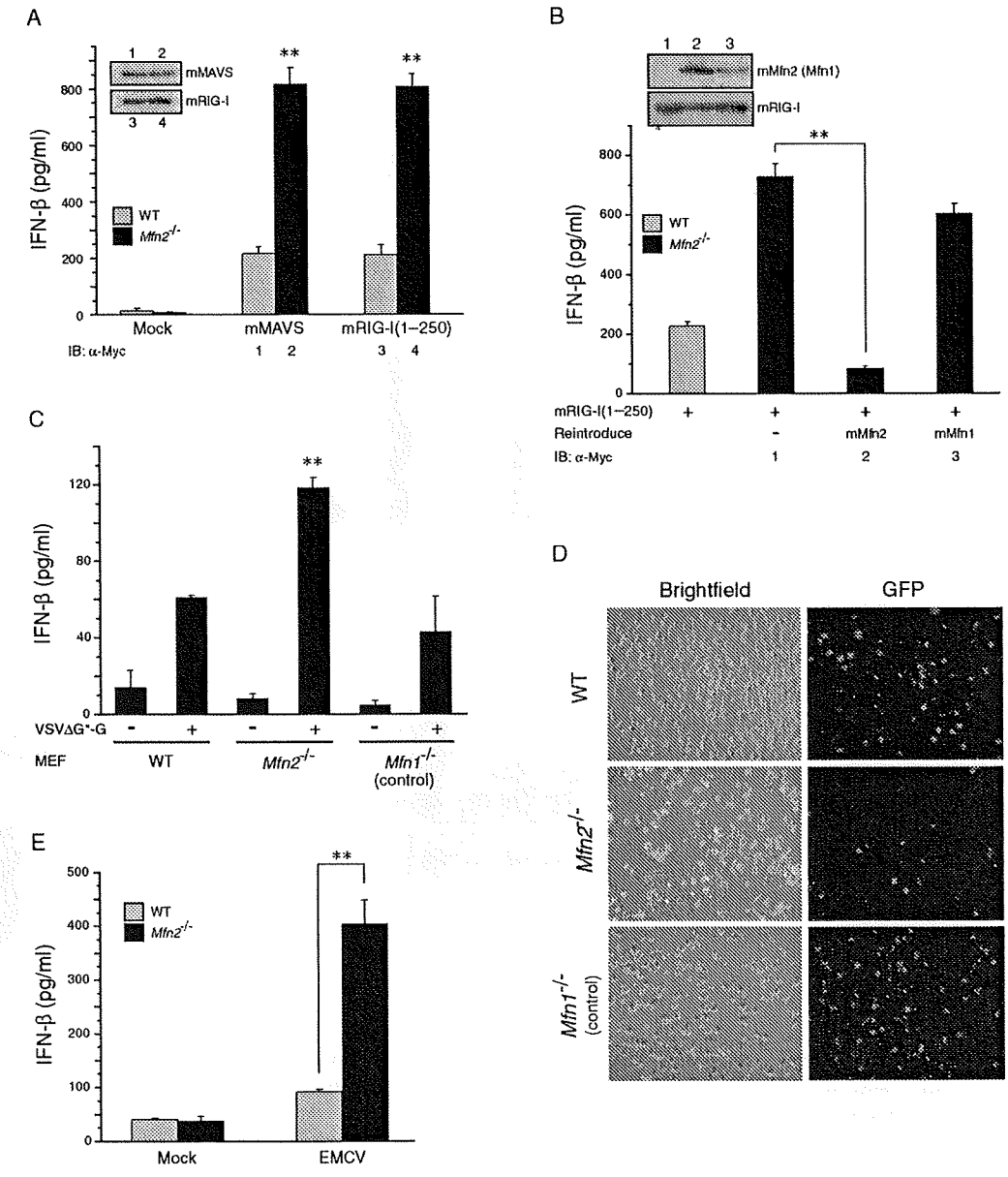

Fig. 5. The effect of Mfn2 deficiency on viral infection in MEFs. (A) WT and *Mfn2*-deficient MEFs were transfected with plasmids encoding either murine MAVS or mRIG-I(1–250), and the production of IFN-β was measured by ELISA 24 hours after transfection. Mock treatment of MEFs involved their transfection with equivalent amounts of pcDNA3.1(–). (B) Reconstitution of *Mfn2*-deficient MEFs with Mfn2 restores modulation of the IFN-β response. *Mfn2*-deficient MEFs were transfected with plasmids encoding mRIG-I(1–250) and either Myc-tagged mMfn2 or mMfn1, and culture supernatants were harvested 24 hours later for measurement of IFN-β production by ELISA. Expression of the plasmids encoding Mfn2 or Mfn1 was confirmed by analysis of Western blots with an antibody against Myc (inset, lanes 2 and 3). (C) This experiment was performed similarly to that described in (A) except that WT and *Mfn2*-deficient MEFs were infected with VSVΔG*-G at an MOI of 3. In this experiment, $Mfn1^{-/-}$ MEFs were also used as a control to evaluate the specificity of Mfn2 in modulating the antiviral response. (D) Fluorescence microscopy (GFP) of MEFs infected with VSVΔG*-G at an MOI of 3 for 24 hours. (E) WT and *Mfn2*-deficient MEFs were infected with EMCV at an MOI of 3, and the production of IFN-β was measured by ELISA. All ELISA data shown represent mean values ± SD ($n = 3$ experiments). $^{**}P < 0.01$.

The HR1 region of Mfn2 is critical for its interaction with MAVS

Through a coimmunoprecipitation approach, we mapped the region of Mfn2 that interacted with MAVS to a central 4,3 hydrophobic heptad repeat (HR1) region (Mfn2-HR1) (Fig. 6A). An analogous approach with deletion mutants of MAVS yielded results indicating that the C-terminal regions of MAVS (amino acid residues 201 to 540) were both necessary and sufficient for the interaction with Mfn2-HR1, and that both the CARD, which is important for the interaction between MAVS and cytoplasmic RNA helicases, and the proline-rich domain were dispensable for this interaction (Fig. 6B). The interaction between Mfn2-HR1 and MAVS was observed only with the transmembrane-anchored form of MAVS (C-term/TM), indicating that the Mfn2-HR1 fragment recognized a structural or topological element (or both) that was specific to the mitochondrial outer membrane–bound form of MAVS.

These results prompted us to investigate the functional role of the HR1 region in the regulation of the antiviral response. In HEK 293 cells, expression of a plasmid encoding the Mfn2-HR1 fragment potently and dose-dependently suppressed IFN-β and NF-κB responses to the overexpression of MAVS-, RIG-I(1–250), and MDA-5 (Fig. 6C and fig. S4) in a manner similar to that observed with full-length Mfn2, indicating that the HR1 region could behave as a dominant-negative modulator of antiviral signaling. Mutations of the predicted *f* position in the HR1 region (E424G and R468H) (fig. S5), which is exposed on the surface of the protein, resulted in a severe loss of function when we evaluated the ability of the mutated protein to modulate the RIG-I–induced IFN-β response, whereas a GTPase mutant of Mfn2 ($Mfn2^{K109A}$) behaved nearly similarly to WT Mfn2 (Fig. 6D). Although the HR1 region has been characterized as an im-

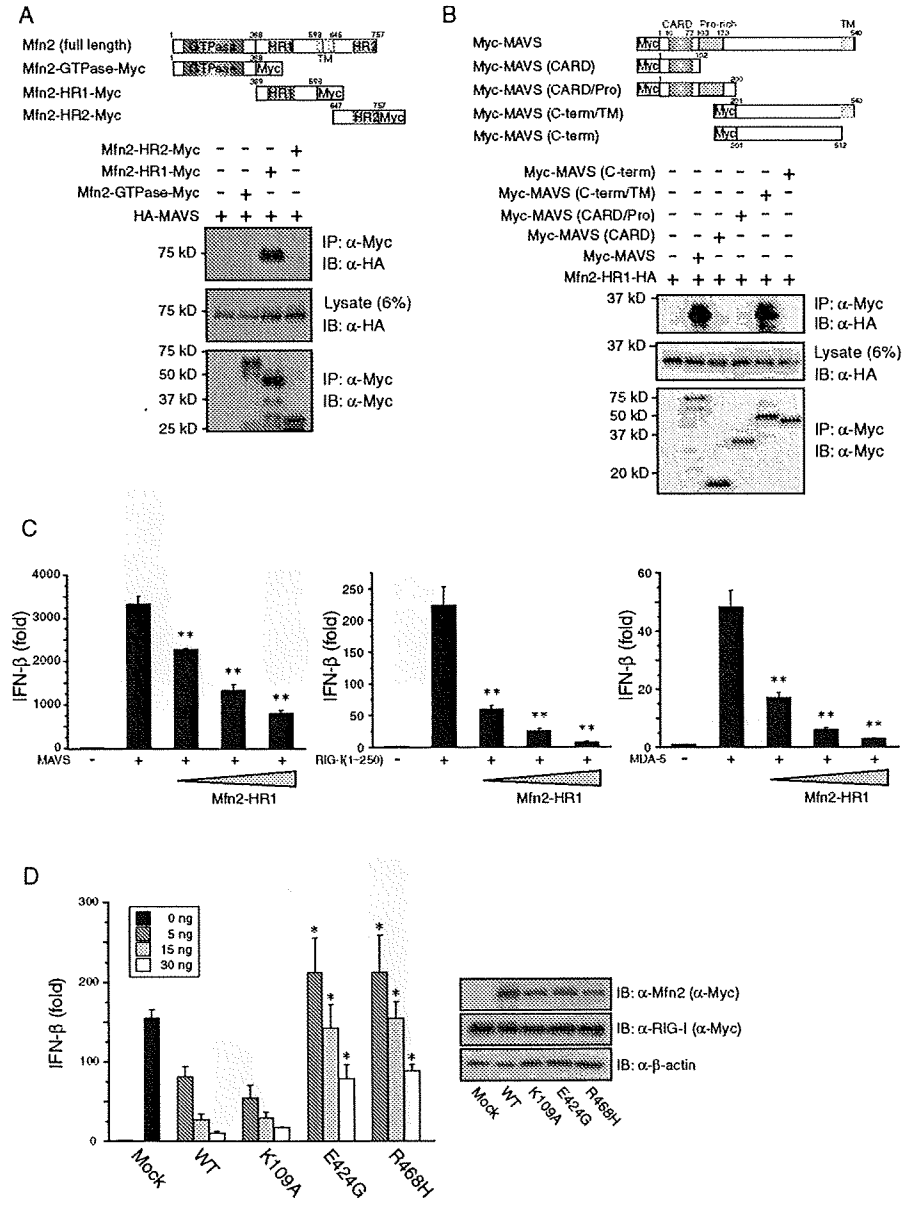

Fig. 6. The HR1 region of Mfn2 associates with MAVS and inhibits activation of the IFN-β reporter. (A) Interaction of HA-tagged MAVS and Myc-tagged Mfn2 variants (upper panel) was analyzed by coimmunoprecipitation assays, which were performed as described for Fig. 1B. The GTPase domain, hydrophobic heptad repeats (HR) 1 and 2, and transmembrane segment (TM) are depicted. (B) Interaction of truncated MAVS variants with the Mfn2-HR1 fragment. (C) HEK 293 cells were cotransfected with 50 ng of plasmids encoding either MAVS, RIG-I(1–250), or MDA-5 together with increasing amounts (20, 50, and 100 ng) of a plasmid encoding the Mfn2-HR1 fragment and the IFN-β luciferase reporter plasmid as described for Fig. 2. (D) HEK 293 cells were cotransfected with 50 ng of plasmid encoding RIG-I(1–250) and increasing amounts (5, 15, and 30 ng; inset) of plasmids encoding WT and mutant Mfn2 proteins together with the IFN-β reporter plasmid. Western blots showing the abundance of the WT and mutant Mfn2 proteins, as well as the abundance of stimulated RIG-I(1–250). All data shown represent mean values ± SD (n = 3 experiments). *P < 0.05; **P < 0.01.

portant domain for mitochondrial targeting (*30*) or fusion (*31*), its functional role in mitofusin homologs is still poorly understood. Our results indicate that the HR1 region of Mfn2 is critical for regulating the antiviral signaling pathway.

Mfn2 functions upstream of TRAF6 and TBK-1

Because Mfn2 was required for regulating antiviral signaling through MAVS, it was likely that Mfn2 acted downstream of (or at the same level as) MAVS in this pathway. In the course of examining the mechanism of its inhibitory activity, we found that Mfn2-specific siRNA had no effect either on the activation of the NF-κB reporter in response to tumor necrosis factor receptor-associated factor 6 (TRAF6) (Fig. 7A), an essential upstream regulator of the inhibitor of κB kinase complex, or on the activation of the IFN-β reporter in response to TANK-binding kinase 1 (TBK-1) (Fig. 7A), a kinase that targets IRF-3, even though both of these effectors act downstream of MAVS (*9*, *15*, *32*, *33*). Consistent with these findings, the production of the proinflammatory cytokine interleukin-6 (IL-6) by TRAF6 was also unaffected in *Mfn2*-deficient MEFs (Fig. 7B), suggesting that Mfn2 inhibited the RIG-I pathway downstream of MAVS and upstream of both TRAF6 (the NF-κB activation pathway) and TBK-1 (the IRF-3 activation pathway).

DISCUSSION

The mitochondrion is well known as the powerhouse of eukaryotic cells, and it is additionally involved in antiviral immunity in vertebrates (*9*–*13*). Despite the central role that the mitochondrial integral membrane protein MAVS plays in this pathway, few additional mitochondrial membrane proteins have been implicated in regulating its activity. In this study, we described our findings that Mfn2, a known mediator of mitochondrial fusion, interacted with MAVS to inhibit antiviral signaling pathways.

Our results show that MAVS forms a stable supramolecular assembly on the outer mitochondrial membrane at physiological pH. We propose that the MAVS complex is an Mfn2-dependent complex because knockdown of endogenous Mfn2 reduced the apparent molecular mass of MAVS, as determined by analytical size exclusion chromatography, from ~600 kD to a lower molecular mass (Fig. 4A). Because loss of endogenous Mfn2 also enhanced the MAVS-mediated antiviral response, it is possible that rearrangement of MAVS from a higher- to a lower-order complex is a prerequisite for the activation of MAVS in response to upstream signaling from RIG-I or MDA-5. Such a model would suggest that Mfn2 functions by stably sequestering MAVS in nonproductive higher-order complexes that are incapable of propagating a downstream antiviral response. A small portion of MAVS did not colocalize with Mfn2, as observed by both size exclusion chromatography (Fig. 4A) and immunofluorescence microscopy (Fig. 1D), raising the possibility that this fraction represents an available pool of MAVS that could be easily activated on viral infection. At present, it is unclear whether the lower-order state is more favorable for recruiting downstream molecules such as TRAF family members or whether it is preferentially competent for signaling to the IRF-3 or NF-κB activation pathways.

In conclusion, we propose a mechanism for the regulation of the cellular antiviral response in which signaling events at the mitochondrial outer membrane involving MAVS are modulated by Mfn2 through its HR1

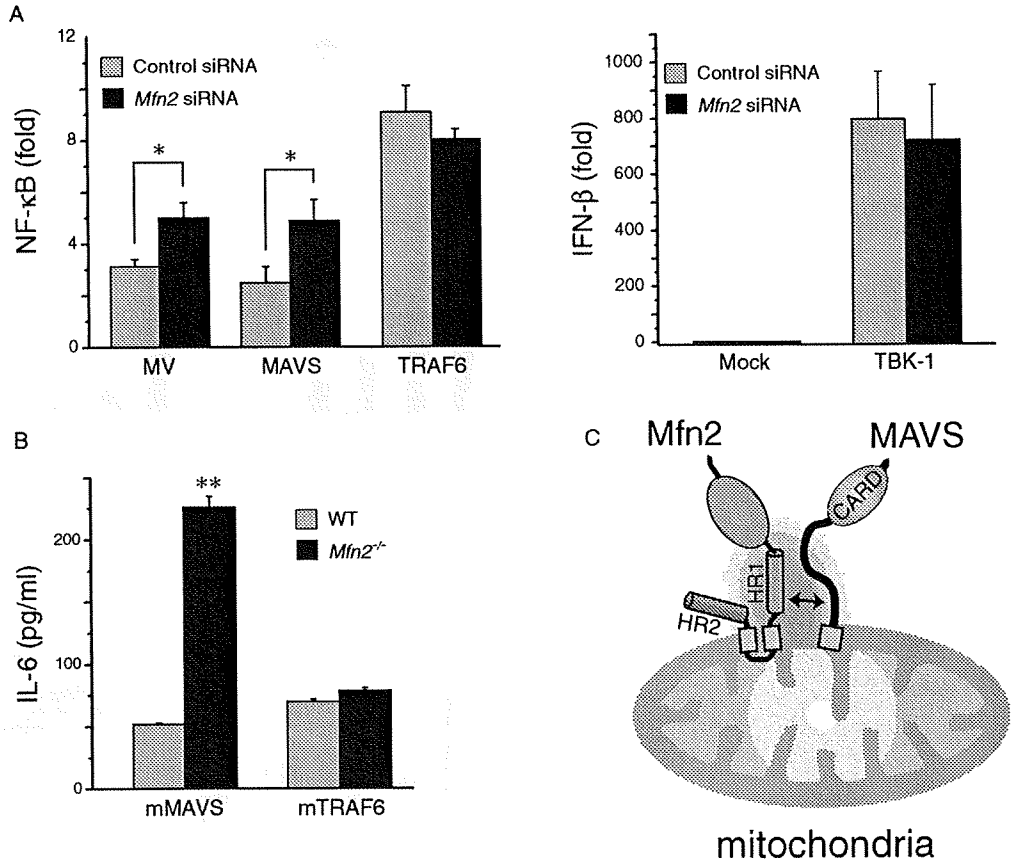

Fig. 7. The role of Mfn2 in antiviral signaling. (A) Activation of NF-κB (left panel) and IFN-β (right panel) reporters in siRNA-treated HEK 293 cells transfected with plasmids encoding MAVS, TRAF6, or TBK-1. In the control (left panel), cells were infected with measles virus (MV) at an MOI of 2. (B) WT and *Mfn2*-deficient MEFs were transfected with plasmids encoding either mMAVS or mTRAF6, and the subsequent production of IL-6 was measured by ELISA. All data shown represent mean values ± SD ($n = 3$ experiments). *$P < 0.05$; **$P < 0.01$. (C) Schematic representation of the MAVS-Mfn2 interaction on the mitochondrial outer membrane.

region (Fig. 7C) upon formation of a supramolecular complex. In this model, we speculate that Mfn2 inhibits the function of the C-terminal region (including the transmembrane domain) of MAVS rather than blocks its CARD, in contrast to previous findings with NOD-like receptor (NLR) family member X1 (NLRX1), a member of the cytoplasmic NLR family that also modulates MAVS-dependent antiviral signaling (*11*). Moreover, it is noteworthy that inhibition of MAVS-mediated antiviral signaling was not observed with Mfn1, which suggests that Mfn1 and Mfn2 are not functionally redundant and illustrates that Mfn2 has multiple specialized functions in the cell (*22–24*, *34*). A small amount of Mfn2 is thought to be present in the ER (*22*). In addition, stimulator of interferon genes (STING) [also termed MITA (*13*)], an essential mediator of the activation of IRF-3, is also present in the ER, mitochondria, or both and interacts with MAVS (*35*). Collectively, these findings raise questions about the interplay between the ER and mitochondria that control antiviral signaling and raise the possibility that Mfn2 may be involved.

MATERIALS AND METHODS

Cell culture

The HEK 293 and HeLa cell lines were maintained in Dulbecco's modified Eagle's medium (DMEM, GIBCO BRL) supplemented with 1% L-glutamine, 1% penicillin-streptomycin, and 10% bovine calf serum or 10% fetal calf serum, respectively, at 5% CO_2 and 37°C. WT, *Mfn1*$^{-/-}$, and *Mfn2*$^{-/-}$ MEFs were provided by D. Chan (Howard Hughes Medical Institute, Caltech) and maintained in standard medium (DMEM supplemented with 10% bovine calf serum) as described previously (*28*). Immunofluorescence microscopy to visualize mitochondria was performed as described previously (*19*, *28*).

Plasmid constructions and mutagenesis

Total messenger RNA (mRNA) from HEK 293 and MEFs was isolated with the TRIzol reagent (Invitrogen) and reverse-transcribed with moloney murine leukemia virus reverse transcriptase (Wako Pure Chemical Industries, Tokyo, Japan). Polymerase chain reaction assays were performed with PrimeSTAR DNA polymerase (Takara, Tokyo, Japan). The following primers (see Supplementary Materials for sequences) were used to generate the complete open reading frames of human MAVS: TK349/TK356; hMfn2: TK365/TK366; hMfn1: TK363/TK364; hFis1: TK367/TK368; hRIG-I(1–250): TK357/TK358; hMDA-5: TK442/TK443; hTBK-1: TK497/TK498; murine MAVS: TK300/TK307; and mRIG-I(1–250): TK310/TK345. Plasmids encoding epitope-tagged MAVS proteins were constructed by ligating the MAVS cDNA into Not I– and Eco RV–digested pcDNA3.1(−) vector (Invitrogen) that encoded either an N-terminal 3× Myc or 3× hemagglutinin (HA) tag. The hMfn2, hMfn1, hRIG-I(1–250), and hMDA-5 cDNAs were ligated into pcDNA3.1 that encoded either a C-terminal 7× Myc or a 3× HA tag.

Antibodies

Antibodies against human MAVS (hMAVS) and murine MAVS (mMAVS) were generated by immunizing rabbits with either recombinant N-terminal histidine-tagged hMAVS (amino acid residues 1 to 175) or mMAVS (amino acid residues 1 to 173), respectively. The recombinant proteins were overexpressed in *Escherichia coli* and purified from solubilized inclusion bodies. The immunoglobulin G (IgG) fractions were affinity-purified with the Econo-Pac Protein A Kit (BioRad). Monoclonal antibodies against Myc (9E10) and HA (HA.11) were purchased from Covance. Monoclonal antibodies against hMfn2, hTom20, IRF-3, and β-actin were obtained from Santa Cruz, and the rabbit monoclonal antibody (4D4G) against phosphorylated IRF-3 (at Ser^{396}) was from Cell Signaling. The Alexa Fluor 568–conjugated monoclonal antibody against mouse IgG was purchased from Molecular Probes. Polyclonal antibody against hFis1 was from ALEXIS Biochemicals. The monoclonal antibody against mitochondrial heat shock protein 70 (mtHsp70) was from Affinity BioReagents. The polyclonal antibody against rat Mfn2 was a gift from K. Mihara (Kyushu University, Japan).

Analytical size exclusion chromatography

Three 10-cm dishes of confluent HEK 293 cells were washed once with cold 1× phosphate-buffered saline (PBS) (pH 7.2), and cells were scraped off and lysed in 1 ml of homogenization buffer [20 mM Hepes (pH 7.5), 70 mM sucrose, and 220 mM mannitol] by 30 strokes in a Dounce homogenizer. The homogenate was centrifuged at 800*g* for 5 min to precipitate nuclei, and the resulting supernatant was further centrifuged at 10,000*g* for 10 min at 4°C to precipitate the crude mitochondrial fraction. After the pellet was washed once with homogenization buffer, the mitochondrial extracts were prepared by solubilization with lysis buffer [50 mM tris-HCl (pH 7.2), 200 mM NaCl, 10% glycerol, and 1% digitonin] and clarification by centrifugation at 12,000*g* for 5 min. Size exclusion chromatography of mitochondrial extracts was performed on Superdex-200 HR-10/30 or Superose 6 HR-10/30 columns (GE Healthcare) equilibrated with 50 mM tris-HCl (pH 7.2) containing 200 mM NaCl, 10% glycerol, and 0.1% NP-40. Extracts were loaded onto the column at a flow rate of 0.3 ml/min at room temperature. Fractions (600 μl each) were collected, resolved by 8% SDS–polyacrylamide gel electrophoresis (SDS-PAGE), and analyzed by Western blotting with either a polyclonal antibody against hMAVS (see above) or a monoclonal antibody against hMfn2. For the analysis of Fis1, fractions were resolved by 15% SDS-PAGE followed by Western blotting analysis with a polyclonal antibody against hFis1. The following molecular weight standards (GE Healthcare) were used: Blue Dextran-2000 (2000 kD), thyroglobulin (669 kD), ferritin (440 kD), catalase (232 kD), and bovine serum albumin (67 kD).

Immunoprecipitation of the hMAVS complex

HEK 293 cells were transfected with the expression plasmid encoding 3× Myc-tagged hMAVS (see above) by the calcium phosphate method. Transfected cells were selected in DMEM medium supplemented with hygromycin B (200 μg/ml; Wako Pure Chemical Industries) for 2 weeks. Stably transfected cells were grown to confluence on five 15-cm dishes. Cells were washed three times with 1× PBS (pH 7.2) and lysed with 10 ml of lysis buffer [20 mM Hepes (pH 7.5), 150 mM NaCl, 10% glycerol, 1 mM EDTA, 1 mM DTT, and 1% digitonin] supplemented with Complete Mini Protease Inhibitor Cocktail (Roche). The clarified supernatant was incubated with monoclonal antibody against the Myc tag (9E10) at 4°C for 2 hours, after which 60 μl of protein A–Sepharose beads (GE Healthcare) was added. After incubation for 5 hours at 4°C, the beads were washed three times with lysis buffer, and immunoprecipitates were resolved by 10% SDS-PAGE. Silver-stained bands were analyzed by LC/MS/MS (Medical Institute of Bioregulation, Kyushu University, Japan).

Coimmunoprecipitations

Coimmunoprecipitation experiments were performed as described previously (*36*) with minor modifications. HEK 293 cells at 80% confluence were transiently transfected with the appropriate plasmids (2 μg each) in a six-well plate by the calcium phosphate method. Two days after transfection, cells were lysed with 1 ml of lysis buffer [50 mM tris-HCl (pH 7.4), 150 mM NaCl, 10% glycerol, and 1% NP-40], and the clarified supernatants were incubated overnight at 4°C with 20 μl of agarose beads (Sigma-Aldrich) conjugated to a polyclonal antibody against *c*-Myc. After four washes with 1× PBS (pH 7.2), immunoprecipitates were resolved by 8 or 12% SDS-PAGE and analyzed by Western blotting with a monoclonal antibody (HA.11) against the HA tag followed by a horseradish peroxidase (HRP)-conjugated antibody against mouse IgG (Jackson ImmunoResearch). To immunoprecipitate endogenous MAVS, HEK 293 cells and MEFs were

lysed with 1% digitonin lysis buffer, and the clarified supernatants were incubated with 10 μg of antibody against hMAVS or mMAVS, followed by incubation overnight at 4°C with 20 μl of protein A–Sepharose beads. The beads were washed four times with lysis buffer, and immunoprecipitates were resolved by 8% SDS-PAGE, analyzed by Western blotting with a monoclonal antibody against hMfn2, and detected with a HRP-conjugated antibody against mouse IgG.

Luciferase assays

HEK 293 cells (2×10^5 cells per well) were plated in 24-well plates. The following day, cells were cotransfected with 100 ng of a luciferase reporter plasmid (p125luc or pELAM), 2.5 ng of the *Renilla* luciferase internal control vector phRL-TK (Promega), and each of the indicated plasmids with the Lipofectamine 2000 reagent (Invitrogen). Empty vector [pcDNA3.1(−)] was used to maintain equivalent amounts of DNA in each well. Cells were harvested 24 hours after transfection and analyzed by a dual-luciferase reporter assay on the GloMax 20/20n luminometer (Promega). Each experiment was replicated at least three times. The p125luc reporter plasmid was provided by T. Taniguchi (University of Tokyo, Japan).

Native PAGE

Native PAGE experiments were performed as described previously (*37*).

RNA interference

For RNA interference–based knockdown experiments, a 25-nucleotide siRNA was purchased from Invitrogen (Stealth Select RNAi). HEK 293 cells were transfected with 50 nM siRNA (final concentration) with Lipofectamine RNAiMAX (Invitrogen). The following day, cells were transfected with luciferase reporter plasmids and then harvested after an additional 24 hours. The designation and sequence (sense strand only) of the Stealth Select RNAi oligonucleotides used in the study were hMfn2 (HSS115028) and 5′-ggaccuccaugggcauucuuguugu-3′, respectively. Stealth RNAi Negative Control Medium GC Duplex #2 (Invitrogen) was used as the control.

ELISA

Production of IFN-β by HEK 293 cells and MEFs was measured with species-specific ELISA reagents for human and murine IFN-β from Kamakura Techno-Science Inc. (Kanagawa, Japan) and PBL Biomedical Laboratories, respectively. The ELISA kit for murine IL-6 was purchased from R&D Systems.

Viral infections

The siRNA-treated HEK 293 cells, which were also cotransfected with reporter plasmids, were plated in 12-well plates and incubated overnight. When the cells were 50% confluent, the culture medium was aspirated and the cells were infected with 200 μl of the Edmonston strain of measles virus (*38*) at 37°C at a multiplicity of infection (MOI) of 2. One hour after infection, cells were supplemented with 800 μl of standard DMEM, then incubated for another 48 hours before the performance of luciferase assays. MEFs were infected with either VSVΔG*-G (*29*) or EMCV (*25*) at an MOI of 3 and incubated for 24 hours before analysis by ELISA, as described above.

SUPPLEMENTARY MATERIALS

www.sciencesignaling.org/cgi/content/full/2/84/ra47/DC1

Materials

Fig. S1. Interaction between endogenous mMfn2 and mMAVS in MEFs.

Fig. S2. Knockdown of Mfn2 with specific siRNA results in enhanced MAVS-mediated activation of the IFN-β reporter.

Fig. S3. Treatment of HEK 293 cells with Mfn2-specific siRNA increased the production of endogenous IFN-β in response to transfection with poly(I:C).

Fig. S4. Mfn2-HR1 is a dominant-negative modulator of MAVS-mediated activation of NF-κB.

Fig. S5. Sequence alignment of Mfn2 homologs within HR1.

Table S1. List of mitochondrial proteins, other than Mfn2, that were identified by LC/MS/MS.

Reference

REFERENCES AND NOTES

1. J. A. Hoffmann, F. C. Kafatos, C. A. Janeway Jr., R. A. B. Ezekowitz, Phylogenetic perspectives in innate immunity. *Science* **284**, 1313–1318 (1999).
2. S. Akira, K. Takeda, T. Kaisho, Toll-like receptors: Critical proteins linking innate and acquired immunity. *Nat. Immunol.* **2**, 675–680 (2001).
3. T. Kawai, S. Akira, Innate immune recognition of viral infection. *Nat. Immunol.* **7**, 131–137 (2006).
4. A. Le Bon, D. F. Tough, Links between innate and adaptive immunity via type I interferon. *Curr. Opin. Immunol.* **14**, 432–436 (2002).
5. A. Iwasaki, R. Medzhitov, Toll-like receptor control of the adaptive immune responses. *Nat. Immunol.* **5**, 987–995 (2004).
6. X. Wang, The expanding role of mitochondria in apoptosis. *Genes Dev.* **15**, 2922–2933 (2001).
7. S. Raha, B. H. Robinson, Mitochondria, oxygen free radicals, disease and ageing. *Trends Biochem. Sci.* **25**, 502–508 (2000).
8. G. A. Rutter, R. Rizzuto, Regulation of mitochondrial metabolism by ER Ca^{2+} release: An intimate connection. *Trends Biochem. Sci.* **25**, 215–221 (2000).
9. R. B. Seth, L. Sun, C. K. Ea, Z. J. Chen, Identification and characterization of MAVS, a mitochondrial antiviral signaling protein that activates NF-κB and IRF3. *Cell* **122**, 669–682 (2005).
10. X. D. Li, L. Sun, R. B. Seth, G. Pineda, Z. J. Chen, Hepatitis C virus protease NS3/4A cleaves mitochondrial antiviral signaling protein off the mitochondria to evade innate immunity. *Proc. Natl. Acad. Sci. U.S.A.* **102**, 17717–17722 (2005).
11. C. B. Moore, D. T. Bergstralh, J. A. Duncan, Y. Lei, T. E. Morrison, A. G. Zimmermann, M. A. Accavitti-Loper, V. J. Madden, L. Sun, Z. Ye, J. D. Lich, M. T. Heise, Z. Chen, J. P. Ting, NLRX1 is a regulator of mitochondrial antiviral immunity. *Nature* **451**, 573–577 (2008).
12. I. Tattoli, L. A. Carneiro, M. Jéhanno, J. G. Magalhaes, Y. Shu, D. J. Philpott, D. Arnoult, S. E. Girardin, NLRX1 is a mitochondrial NOD-like receptor that amplifies NF-κB and JNK pathways by inducing reactive oxygen species production. *EMBO Rep.* **9**, 293–300 (2008).
13. B. Zhong, Y. Yang, S. Li, Y. Y. Wang, Y. Li, F. Diao, C. Lei, X. He, L. Zhang, P. Tien, H. B. Shu, The adaptor protein MITA links virus-sensing receptors to IRF3 transcription factor activation. *Immunity* **29**, 538–550 (2008).
14. T. Kawai, K. Takahashi, S. Sato, C. Coban, H. Kumar, H. Kato, K. J. Ishii, O. Takeuchi, S. Akira, IPS-1, an adaptor triggering RIG-I- and Mda5-mediated type I interferon induction. *Nat. Immunol.* **6**, 981–988 (2005).
15. L. G. Xu, Y. Y. Wang, K. J. Han, L. Y. Li, Z. Zhai, H. B. Shu, VISA is an adapter protein required for virus-triggered IFN-β signaling. *Mol. Cell* **19**, 727–740 (2005).
16. E. Meylan, J. Curran, K. Hofmann, D. Moradpour, M. Binder, R. Bartenschlager, J. Tschopp, Cardif is an adaptor protein in the RIG-I antiviral pathway and is targeted by hepatitis C virus. *Nature* **437**, 1167–1172 (2005).
17. H. Kumar, T. Kawai, H. Kato, S. Sato, K. Takahashi, C. Coban, M. Yamamoto, S. Uematsu, K. J. Ishii, O. Takeuchi, S. Akira, Essential role of IPS-1 in innate immune responses against RNA viruses. *J. Exp. Med.* **203**, 1795–1803 (2006).
18. Q. Sun, L. Sun, H. H. Liu, X. Chen, R. B. Seth, J. Forman, Z. J. Chen, The specific and essential role of MAVS in antiviral innate immune responses. *Immunity* **24**, 633–642 (2006).
19. A. Jofuku, N. Ishihara, K. Mihara, Analysis of functional domains of rat mitochondrial Fis1, the mitochondrial fission-stimulating protein. *Biochem. Biophys. Res. Commun.* **333**, 650–659 (2005).
20. D. C. Chan, Mitochondrial fusion and fission in mammals. *Annu. Rev. Cell Dev. Biol.* **22**, 79–99 (2006).
21. A. Santel, S. Frank, B. Gaume, M. Herrler, R. J. Youle, M. T. Fuller, Mitofusin-1 protein is a generally expressed mediator of mitochondrial fusion in mammalian cells. *J. Cell Sci.* **116**, 2763–2774 (2003).
22. O. M. de Brito, L. Scorrano, Mitofusin 2 tethers endoplasmic reticulum to mitochondria. *Nature* **456**, 605–610 (2008).
23. K. H. Chen, X. Guo, D. Ma, Y. Guo, Q. Li, D. Yang, P. Li, X. Qiu, S. Wen, R. P. Xiao, J. Tang, Dysregulation of HSG triggers vascular proliferative disorders. *Nat. Cell Biol.* **6**, 872–883 (2004).
24. S. Züchner, I. V. Mersiyanova, M. Muglia, N. Bissar-Tadmouri, J. Rochelle, E. L. Dadali, M. Zappia, E. Nelis, A. Patitucci, J. Senderek, Y. Parman, O. Evgrafov, P. D. Jonghe, Y. Takahashi, S. Tsuji, M. A. Pericak-Vance, A. Quattrone, E. Battologlu, A. V. Polyakov, V. Timmerman, J. M. Schröder, J. M. Vance, Mutations in the mitochondrial GTPase mitofusin 2 cause Charcot-Marie-Tooth neuropathy type 2A. *Nat. Genet.* **36**, 449–451 (2004).

25. M. Yoneyama, M. Kikuchi, T. Natsukawa, N. Shinobu, T. Imaizumi, M. Miyagishi, K. Taira, S. Akira, T. Fujita, The RNA helicase RIG-I has an essential function in double- stranded RNA-induced innate antiviral responses. *Nat. Immunol.* **5**, 730–737 (2004).
26. L. Gitlin, W. Barchet, S. Gilfillan, M. Cella, B. Beutler, R. A. Flavell, M. S. Diamond, M. Colonna, Essential role of mda-5 in type I IFN responses to polyriboinosinic: Polyribocytidylic acid and encephalomyocarditis picornavirus. *Proc. Natl. Acad. Sci. U.S.A.* **103**, 8459–8464 (2006).
27. H. Kato, O. Takeuchi, S. Sato, M. Yoneyama, M. Yamamoto, K. Matsui, S. Uematsu, A. Jung, T. Kawai, K. J. Ishii, O. Yamaguchi, K. Otsu, T. Tsujimura, C. S. Koh, C. Reis e Sousa, Y. Matsuura, T. Fujita, S. Akira, Differential roles of MDA5 and RIG-I helicases in the recognition of RNA viruses. *Nature* **441**, 101–105 (2006).
28. H. Chen, S. A. Detmer, A. J. Ewald, E. E. Griffin, S. E. Fraser, D. C. Chan, Mitofusins Mfn1 and Mfn2 coordinately regulate mitochondrial fusion and are essential for embryonic development. *J. Cell Biol.* **160**, 189–200 (2003).
29. A. Takada, C. Robison, H. Goto, A. Sanchez, K. G. Murti, M. A. Whitt, Y. Kawaoka, A system for functional analysis of Ebola virus glycoprotein. *Proc. Natl. Acad. Sci. U.S.A.* **94**, 14764–14769 (1997).
30. M. Rojo, F. Legros, D. Chateau, A. Lombès, Membrane topology and mitochondrial targeting of mitofusins, ubiquitous mammalian homologs of the transmembrane GTPase Fzo. *J. Cell Sci.* **115**, 1663–1674 (2002).
31. E. E. Griffin, D. C. Chan, Domain interactions within Fzo1 oligomers are essential for mitochondrial fusion. *J. Biol. Chem.* **281**, 16599–16606 (2006).
32. S. M. McWhirter, B. R. Tenoever, T. Maniatis, Connecting mitochondria and innate immunity. *Cell* **122**, 645–647 (2005).
33. R. Yoshida, G. Takaesu, H. Yoshida, F. Okamoto, T. Yoshioka, Y. Choi, S. Akira, T. Kawai, A. Yoshimura, T. Kobayashi, TRAF6 and MEKK1 play a pivotal role in the RIG-I-like helicase antiviral pathway. *J. Biol. Chem.* **283**, 36211–36220 (2008).
34. S. Pich, D. Bach, P. Briones, M. Liesa, M. Camps, X. Testar, M. Palacin, A. Zorzano, The Charcot-Marie-Tooth type 2A gene product, Mfn2, up-regulates fuel oxidation through expression of OXPHOS system. *Hum. Mol. Genet.* **14**, 1405–1415 (2005).
35. H. Ishikawa, G. N. Barber, STING is an endoplasmic reticulum adaptor that facilitates innate immune signalling. *Nature* **455**, 674–678 (2008).
36. T. Koshiba, S. A. Detmer, J. T. Kaiser, H. Chen, J. M. McCaffery, D. C. Chan, Structural basis of mitochondrial tethering by mitofusin complexes. *Science* **305**, 858–862 (2004).
37. T. Iwamura, M. Yoneyama, K. Yamaguchi, W. Suhara, W. Mori, K. Shiota, Y. Okabe, H. Namiki, T. Fujita, Induction of IRF-3/-7 kinase and NF-κB in response to double-stranded RNA and virus infection: Common and unique pathways. *Genes Cells* **6**, 375–388 (2001).
38. Y. Yanagi, M. Takeda, S. Ohno, Measles virus: Cellular receptors, tropism and pathogenesis. *J. Gen. Virol.* **87**, 2767–2779 (2006).
39. We are grateful to D. Chan (Howard Hughes Medical Institute and California Institute of Technology, Pasadena, CA) for helpful discussions and for providing wild-type, *Mfn1*-, and *Mfn2*-deficient MEF cell lines. We are also grateful to J. Kulman (Puget Sound Blood Center, Seattle, WA) and K. Mihara (Kyushu University, Japan) for their valuable comments on the study. We thank M. Matsumoto and M. Oda (Kyushu University) for the LC/MS/MS analysis, and Y. Fuchigami for technical assistance with DNA sequencing. The p125luc reporter plasmid was provided by T. Taniguchi (University of Tokyo, Japan). We also thank A. Yoshimura and T. Kobayashi (Keio University, Japan) for providing the FLAG-mTRAF6 expression plasmid, and T. Fujita and M. Yoneyama (Kyoto University, Japan) for EMCV. K.Y. was supported by an Academic Challenge grant by Venture Business Laboratory, Kyushu University. This work was supported by the grants-in-aid for Young Scientists (B) from the Ministry of Education, Culture, Sports, Science, and Technology of Japan (20770123), Kyushu University Interdisciplinary Programs in Education and Projects in Research Development (P & P type D; 20301), and The Uehara Memorial Foundation to T.K. The authors declare that they have no conflict of interest.

Submitted 24 February 2009
Accepted 31 July 2009
Final Publication 18 August 2009
10.1126/scisignal.2000287
Citation: K. Yasukawa, H. Oshiumi, M. Takeda, N. Ishihara, Y. Yanagi, T.Seya, S. Kawabata, T. Koshiba, Mitofusin 2 inhibits mitochondrial antiviral signaling. *Sci. Signal.* **2**, ra47 (2009).

JOURNAL OF VIROLOGY, Nov. 2009, p. 11996–12001 Vol. 83, No. 22
0022-538X/09/$12.00 doi:10.1128/JVI.00791-09

A Highly Attenuated Measles Virus Vaccine Strain Encodes a Fully Functional C Protein[▽]

Yuichiro Nakatsu,§ Makoto Takeda,§* Masaharu Iwasaki, and Yusuke Yanagi

Department of Virology, Faculty of Medicine, Kyushu University, 3-1-1 Maidashi, Higashi-ku, Fukuoka 812-8582, Japan

Received 20 April 2009/Accepted 20 August 2009

The P, V, and C proteins of measles virus are encoded in overlapping reading frames of the P gene, which makes it difficult to analyze the functions of the individual proteins in the context of virus infection. We established a system to analyze the C protein independently from the P and V proteins by placing its gene in an additional transcription unit between the H and L genes. Analyses with this system indicated that a highly attenuated Edmonston lineage vaccine strain encodes a fully functional C protein, and the P and/or V protein is involved in the attenuated phenotype.

Measles is a highly contagious disease characterized by high fever and a maculopapular rash. About 4% of deaths in children aged under 5 years are caused by measles worldwide (9). The causative agent, measles virus (MV), belongs to the genus *Morbillivirus* in the family *Paramyxoviridae*. The genome of MV is a nonsegmented negative-strand RNA of ~16 kb in length and contains six genes. Each gene encodes a single structural protein, namely the nucleocapsid (N), phospho (P), matrix (M), fusion (F), hemagglutinin (H), and large (L) proteins (17). The genome forms a helical ribonucleoprotein complex with the N protein and viral RNA-dependent RNA polymerase composed of the P and L proteins. The P protein acts as an essential cofactor of RNA-dependent RNA polymerase and tethers the L protein onto the nucleocapsid template (20). The P gene encodes additional gene products, the V and C proteins, by the processes of RNA editing and alternative translational initiation in a different reading frame, respectively (17). Although the V and C proteins are nonessential for MV replication (29, 35), they act as important virulence factors in vivo (11, 28, 44–46). Many lines of evidence have indicated that the C and V proteins of MV antagonize the host interferon (IFN) responses (10, 16, 22, 23, 25, 26, 37, 42, 47). The V protein directly interferes with pathways of IFN induction (1) and IFN signaling (25, 26, 42), while the C protein contributes to circumvention of IFN induction by controlling the levels of viral RNA synthesis (22, 23, 31). Direct interference with IFN signaling by the C protein has also been reported, although its effects are weaker than those of the V protein (16, 37).

In a recent study, we showed that a recombinant IC-B strain possessing the P gene of the attenuated Edmonston tag strain (IC/EdP) replicates less efficiently than the parental IC-B strain (a virulent strain) (40). The Edmonston tag strain is a recombinant MV derived from the Edmonston B vaccine strain, which has been passaged numerous times in various cultured cells (30). There are many amino acid differences between the P gene products of the IC-B and Edmonston tag strains (Fig. 1) (27, 30, 43). Most of the changes found in the Edmonston tag strain are common to the Edmonston lineage MV strains (27). However, owing to two amino acid substitutions at positions 110 and 272, which are not conserved among the Edmonston lineage MV strains (25–27), the V protein of the Edmonston tag strain is defective in counteracting IFN signaling (10, 12, 16, 25). The changes at these two positions are also found in other lineages of MV vaccine strains as well as cultured, cell-adapted MV strains (2, 8, 40). Therefore, we consider the P gene of the Edmonston tag strain to be a representative P gene encoded in attenuated MV strains.

The C protein expressed from the newly created C gene supports MV replication efficiently. Previous studies using expression plasmids have suggested that functional differences in the C protein are possibly involved in the attenuated phenotypes of the Edmonston and vaccine strains of MV (3, 24, 31). These observations motivated us to compare the C protein functions between the IC-B and Edmonston tag strains in the context of virus infection. It should be noted that the licensed, highly attenuated Zagreb vaccine strain encodes a C protein with an amino acid sequence identical to that of the Edmonston tag strain (4, 27). However, analyses of the C protein using infectious MVs pose the problem that mutations in the C protein are often accompanied by mutations in the P and V proteins because they are encoded in overlapping reading frames. In the present study, we established a reverse-genetics system to analyze the C protein independently from the P and V proteins by placing its gene in an additionally created transcription unit (termed the C gene) between the H and L genes (Fig. 2A). The expression levels of MV mRNAs decrease progressively from the 3′ end to the 5′ end of the virus genome. Although the C protein is expressed from the P gene (the second locus of the virus genome) in the original virus genome, the expression level is relatively low. It is because the C protein is translated using the second AUG codon in the P gene transcripts via a leaky scanning mechanism. We, therefore, placed the C gene at a downstream locus (between the H and L genes)

* Corresponding author. Mailing address: Department of Virology, Faculty of Medicine, Kyushu University, 3-1-1 Maidashi, Higashi-ku, Fukuoka 812-8582, Japan. Phone: 81-92-642-6138. Fax: 81-92-642-6140. E-mail: mtakeda@nih.go.jp.

§ Present address: National Institute of Infectious Diseases, Musashimurayama, Tokyo 208-0011, Japan.

▽ Published ahead of print on 2 September 2009.

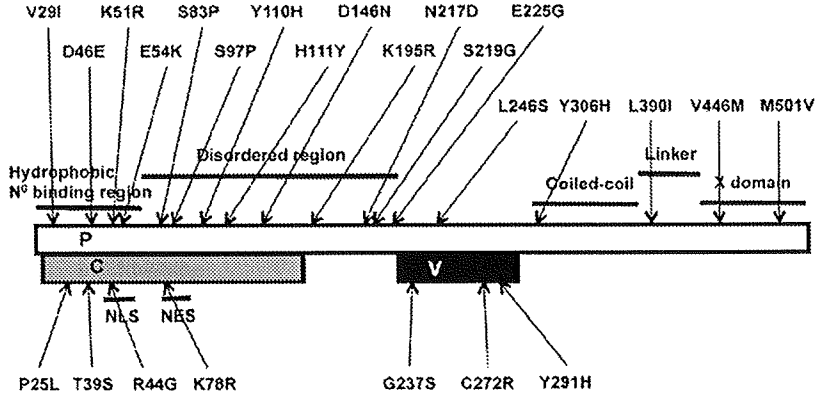

FIG. 1. Amino acid differences between the P, C, and V proteins of the Edmonston tag strain and those of the IC-B strain. The white, gray, and black boxes indicate the reading frames for the P protein and the C protein and the unique carboxyl terminus of the V protein of the Edmonston tag strain, respectively. Substitutions in the P protein compared with the IC-B strain are shown above the boxes, while those in the C and V proteins are shown below the boxes. The functional domains of the P protein (20) are shown as black lines above the white box, while those of the C protein (24) are shown below the gray box. NLS, nuclear localization signal; NES, nuclear export signal.

of the virus genome in order to achieve an expression level of the C protein similar to that from the P gene. The original reading frame of the C protein in the P gene was knocked out by introducing nonsense mutations into the frame, as reported previously (22, 44), and the mutated P gene was termed PΔC. A recombinant MV IC-B strain possessing a genome with these alterations was generated by reverse-genetics techniques (39, 41) and designated ICΔC-add[IC-C] (the C protein of the IC-B strain was termed IC-C). Another recombinant MV, designated ICΔC-add[ΔC], was also generated. This second recombinant MV possessed the C gene but lacked C protein expression owing to introduced nonsense mutations. A third recombinant MV, ICΔC, which lacks C protein expression from the P gene and does not have an additional C gene, has already been reported (22, 44). All the recombinant MV strains analyzed in the present study were derived from IC323-EGFP (18) (termed the wild-type [wt] virus in this study), which was engineered to express enhanced green fluorescent protein (EGFP) from another additional transcriptional unit at the first locus of the genome of the IC-B strain (Fig. 2A) (18). A pulse-labeling experiment revealed that the expression levels of the C protein from the newly created C gene at 24 h postinfection (p.i.) in Vero/hSLAM and A549/hSLAM cells were similar to those from the original P gene (Fig. 2B).

Our previous studies indicated that IFN regulatory factor 3 (IRF3) is activated in cells infected with ICΔC, leading to the production of IFN (22, 23). Furthermore, protein translation is inhibited in these cells through phosphorylation of the eukaryotic translation initiation factor eIF-2α (22). Consequently, ICΔC replicates poorly in these cells possessing a functional IFN system but replicates fairly well in cells with a defective IFN system (22). As observed in ICΔC-infected cells, IRF3 was translocated into the nucleus in ICΔC-add[ΔC]-infected cells, whereas it was hardly translocated into the nucleus in ICΔC-add[IC-C]-infected cells (Fig. 2C). Synthesis of viral proteins was restored in ICΔC-add[IC-C]-infected cells (Fig. 2D). Furthermore, this Western blot analysis reconfirmed the similar expression levels of the C protein for the wt and ICΔC-add[IC-C] viruses at 24 h p.i. (Fig. 2D). ICΔC-add[IC-C] replicated efficiently, and its maximum virus titer was as high as that of the wt virus (Fig. 2E). However, the virus titer of ICΔC-add[IC-C] dropped off more rapidly than that of the wt virus (Fig. 2E), revealing some differences between the growth kinetics of the wt and ICΔC-add[IC-C] viruses at the late stage of virus infection. The rapid decrease in the virus titer of ICΔC-add[IC-C] may thus suggest some difference in the expression levels of the C protein between ICΔC-add[IC-C] and wt viruses after 48 h p.i. Nevertheless, all the data indicate that the C protein expressed from the newly created C gene efficiently supports virus replication similar to that of the C protein expressed from the original P gene.

The C protein of the Edmonston tag strain supports MV replication as efficiently as the wt C protein. Next, the function of the C protein of the Edmonston tag strain (Ed-C) was compared with that of IC-C using the newly developed recombinant virus system with the inserted C gene. Recombinant ICΔC-add[Ed-C], which encodes the C gene of Ed-C, was generated. Synthesis of viral RNAs in either ICΔC-add[IC-C]- or ICΔC-add[Ed-C]-infected cells was controlled to a level similar to that in wt virus-infected cells, whereas it was accelerated in ICΔC-add[ΔC]-infected cells, as observed in ICΔC-infected cells (Fig. 3A). No significant differences were found between the intracellular distribution patterns of Ed-C and IC-C in virus-infected cells (Fig. 3B). IRF3 was hardly translocated into the nucleus in ICΔC-add[Ed-C]-infected cells (Fig. 3C). In addition, ICΔC-add[Ed-C] produced levels of viral proteins similar to those of ICΔC-add[IC-C] (Fig. 3D). Consequently, ICΔC-add[Ed-C] replicated as efficiently as ICΔC-add[IC-C] (Fig. 3E). These data indicate that Ed-C is fully functional in supporting virus replication and circumventing host IFN responses, similar to IC-C. These results are consistent with our previous observation that the ability of the C protein to inhibit viral RNA synthesis is correlated with the abilities of MV to circumvent IFN induction and support virus growth in IFN-competent cells (23). Many studies regarding the roles of the MV C protein in virus replication and pathogenesis have been carried out using the Edmonston tag strain (7, 15, 28, 29, 46). Our present study helps to validate the

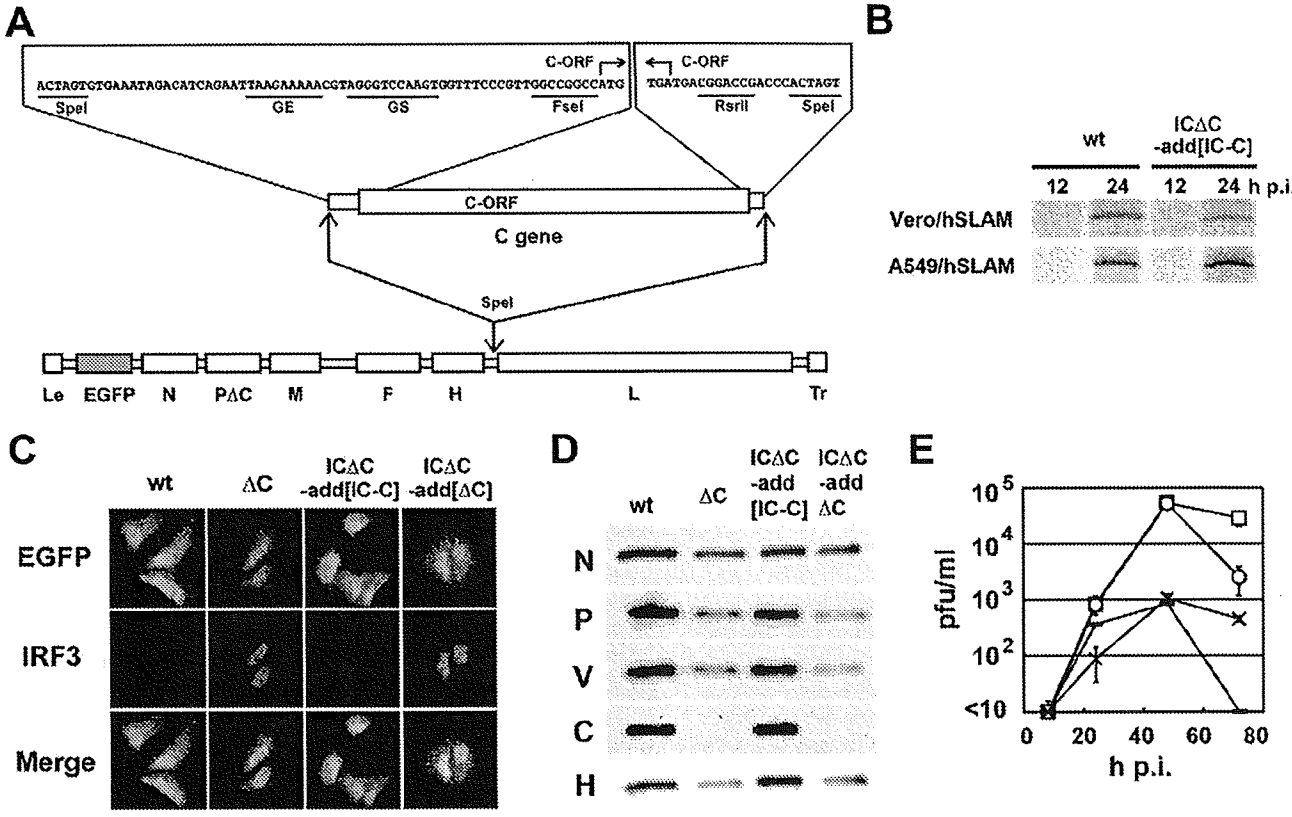

FIG. 2. The C protein expressed from the newly created C gene is fully functional in supporting MV replication. (A) Insertion of an additional transcription unit (the C gene) between the H and L genes. Transcription regulatory regions (gene end [GE], intergenic, and gene start [GS] sequences) and the coding sequence for the C protein (C-ORF) were inserted at the junction between the H and L genes using appropriate restriction enzyme recognition sites (SpeI, FseI, and RsrII). The recombinant MV genome also possesses a transcription unit for EGFP (green). Le and Tr indicate leader and trailer sequence, respectively. (B) Vero/hSLAM and A549/hSLAM cells were infected with wt and ICΔC-add[IC-C] viruses at a multiplicity of infection (MOI) of 0.5. At 12 and 24 h p.i., the cells were pulse-labeled with [^{35}S]methionine-cysteine. The C proteins were immunoprecipitated with an anti-C protein monoclonal antibody (2D10) (23), subjected to sodium dodecyl sulfate-polyacrylamide gel electrophoresis (SDS-PAGE), and detected using a Fuji BioImager 1000 (Fuji, Tokyo, Japan). (C) Indirect immunofluorescence assay for IRF3. A549/hSLAM cells were infected with recombinant MVs (wt, ICΔC, ICΔC-add[IC-C], and ICΔC-add[ΔC]), which express EGFP (18), at an MOI of 0.5 and incubated in medium containing a fusion-blocking peptide (32). At 36 h p.i., IRF3 was detected by an indirect immunofluorescence assay. Green and red fluorescence indicate EGFP encoded in the recombinant MV genome and IRF3, respectively. (D) Expression of viral proteins. A549/hSLAM cells were infected with recombinant MVs at an MOI of 0.5. At 24 h p.i., the N, P, V, C, and H proteins in the cells were detected by SDS-PAGE and Western blotting using appropriate primary and secondary antibodies. (E) Growth kinetics. Monolayers of A549/hSLAM cells were infected with recombinant MVs (□, wt; ×, ICΔC; ○, ICΔC-add[IC-C]; –, ICΔC-add[ΔC]) at an MOI of 0.01. At various time intervals, the infectious virus titers were determined by plaque assays. Data represent the means ± standard deviations (SD) of results from triplicate samples.

knowledge regarding the functions of the C protein obtained using the Edmonston tag strain.

The P/V protein of the Edmonston tag strain is responsible for the attenuated phenotype. None of the data showed any functional differences between IC-C and Ed-C. Consequently, the reduction in virus growth observed for IC/EdP (40) should be caused by the P and/or V (P/V) protein of the Edmonston tag strain. The P gene of the Edmonston tag strain in which C protein expression was knocked out (EdPΔC) was introduced into the ICΔC-add[IC-C] and ICΔC-add[Ed-C] genomes to replace PΔC. The generated viruses were termed IC/EdPΔC-add[IC-C] and IC/EdPΔC-add[Ed-C], respectively. Recombinant MVs possessing EdPΔC (IC/EdPΔC-add[IC-C] and IC/EdPΔC-add[Ed-C]) synthesized smaller amounts of viral RNAs (Fig. 4A) and replicated less efficiently (Fig. 4B) than those possessing PΔC (ICΔC-add[IC-C] and ICΔC-add[Ed-C]). In addition, MVs possessing EdPΔC, including the Edmonston strain and IC/EdP, produced smaller plaques than those possessing PΔC (Fig. 4C) (40). These data confirm that the attenuated growth of IC/EdP is caused by the P/V protein of the Edmonston tag strain and not by the C protein. It is unlikely that the inability of the V protein of the Edmonston tag strain to counteract IFN signaling (10, 12, 16, 25) is associated with the growth attenuation of MV possessing EdPΔC, because we used Vero cells that are defective in the IFN system (14, 21) in these analyses.

Implications. The mechanisms involved in the attenuation of the Edmonston and vaccine strains of MV remain to be elucidated. MV can be attenuated through adaptation to growth in cultured cells (19), and the Edmonston and vaccine strains have been generated through large numbers of passages in various cultured cells (34). Mutations in the P gene are often

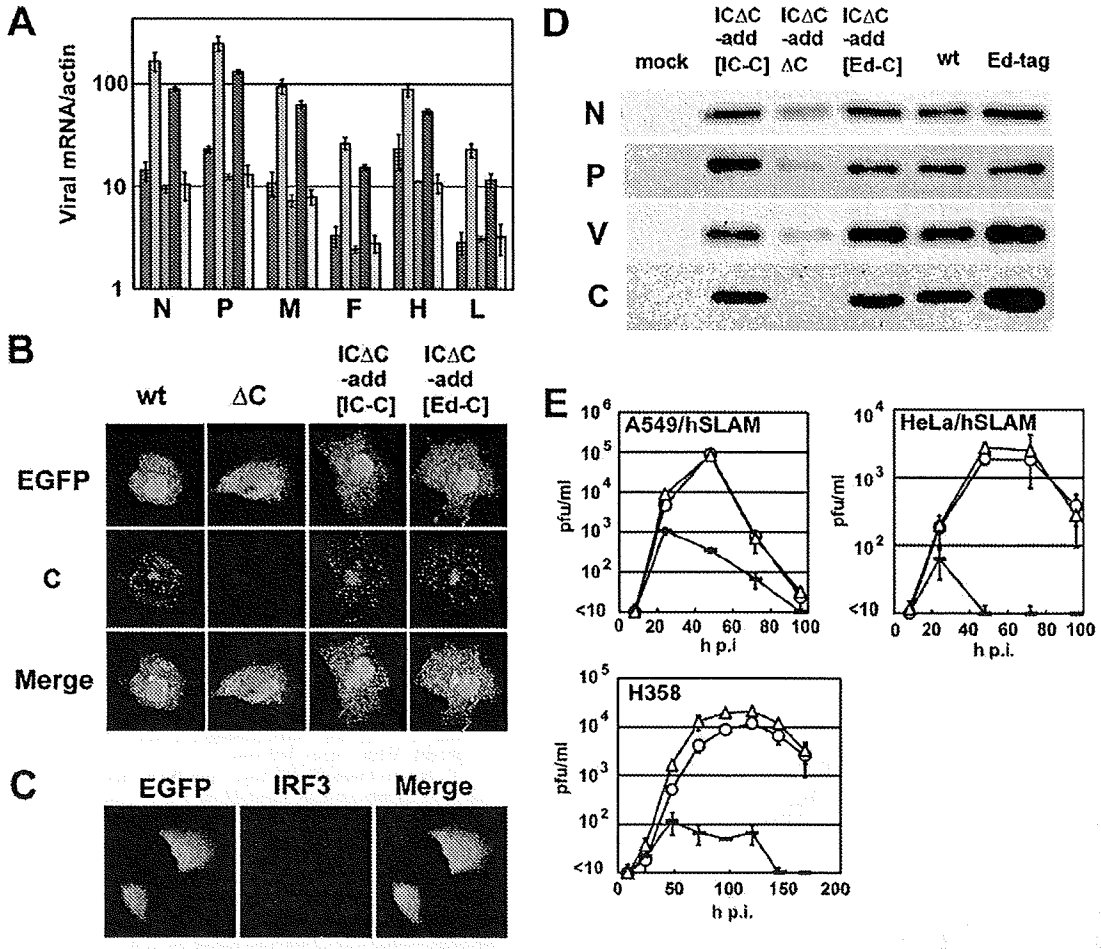

FIG. 3. The C protein of the Edmonston tag strain is equivalent in functionality to the C protein of the IC-B strain. (A) Quantification of viral mRNAs. Vero/hSLAM cells were infected with recombinant MVs (red, wt; light blue, ICΔC; purple, ICΔC-add[IC-C]; blue, ICΔC-add[ΔC]; yellow, ICΔC-add[Ed-C]) at an MOI of 0.5. At 36 h p.i., the viral mRNA levels in the cells were analyzed by reverse transcription-quantitative PCR as previously described (23). Data represent the means ± SD of results from triplicate samples. (B) Intracellular distribution of the C protein. Vero/hSLAM cells were infected with recombinant MVs expressing EGFP (18) at an MOI of 0.5 in the presence of a fusion-blocking peptide (32). At 36 h p.i., the intracellular distribution of the C protein was analyzed by an indirect immunofluorescence assay using appropriate primary and secondary antibodies (23). Green and red fluorescence indicate EGFP encoded in the recombinant MV genome and the C protein, respectively. (C) Indirect immunofluorescence assay for IRF3. ICΔC-add[Ed-C]-infected A549/hSLAM cells were subjected to an indirect immunofluorescence assay for IRF3 using the same procedures described in the legend for Fig. 2C. (D) Expression of viral proteins. Viral proteins in recombinant MV-infected A549/hSLAM cells were detected using the same procedures described in the legend for Fig. 2D. (E) Growth kinetics. Monolayers of A549/hSLAM, HeLa/hSLAM, and H358 cells were infected with recombinant MVs (○, ICΔC-add[IC-C]; ●, ICΔC-add[ΔC]; △, ICΔC-add[Ed-C]) at an MOI of 0.01. At various time intervals, the infectious virus titers were determined by plaque assays. Data represent the means ± SD of results from triplicate samples.

observed during the adaptation process of MV (2, 13, 27, 38, 43) as well as in related viruses (5, 6, 33). The C protein was shown to be dispensable for virus growth in some cultured cells (29) but acts as an important virulence factor in vivo (11, 28, 44). Therefore, mutations in the C protein are possibly responsible for the attenuated phenotypes of the Edmonston and vaccine strains of MV. However, recent studies have indicated that the C protein plays important roles in circumventing the host innate immune responses (16, 22, 23, 37, 47) and is therefore dispensable for virus growth in cultured cells only when the cells have a defective IFN system (15, 22, 44). Our data indicate that Ed-C is fully functional in supporting virus growth in cells possessing a functional IFN system. Preservation of a functional C protein by the Edmonston tag and vaccine strains of MV would be reasonable, since they have to grow in chicken embryo fibroblasts (34), which possess an intact IFN system (36).

It has long been believed that the Edmonston strain and its derivative vaccines have acquired mutations that may promote viral RNA synthesis in cultured cells. However, this is unlikely to be the case. Our present data suggest that the P/V protein of the Edmonston tag strain attenuates MV growth by reducing the level of viral RNA synthesis. We speculate that this may allow the virus to circumvent the host innate immune responses effectively, thereby leading to better survival in various cultured cells. Our present data

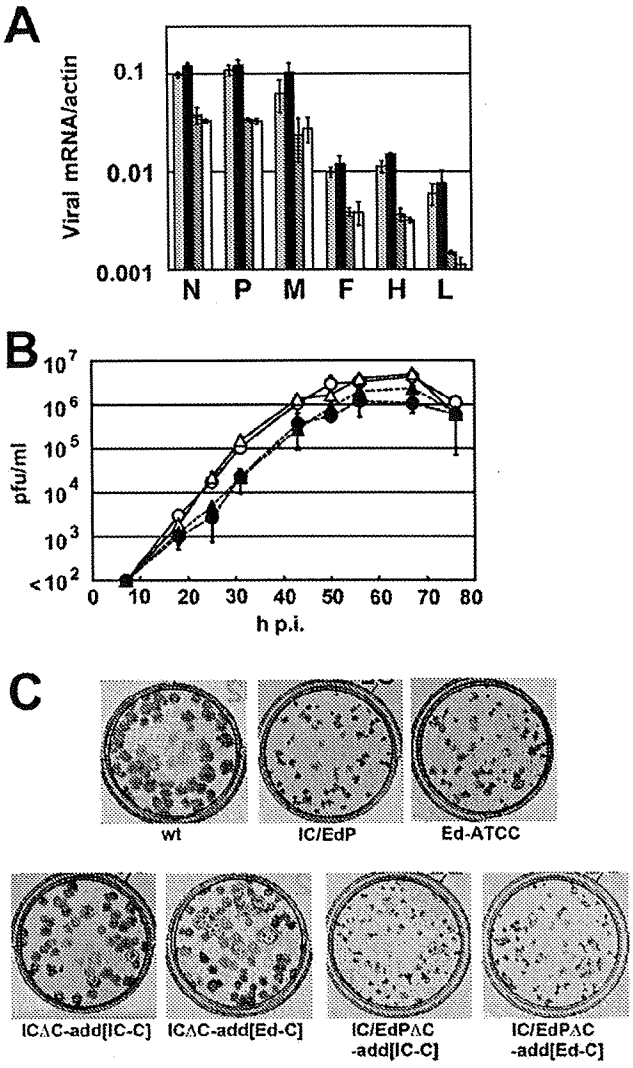

FIG. 4. The P/V protein, but not the C protein, attenuates MV RNA synthesis and growth. (A) Quantification of viral mRNAs. Monolayers of Vero/hSLAM cells were infected with recombinant MVs (light gray, ICΔC-add[IC-C]; black, ICΔC-add[Ed-C]; dark gray, IC/EdPΔC-add[IC-C]; white, IC/EdPΔC-add[Ed-C]) at an MOI of 0.01 in the presence of a fusion-blocking peptide (32). At 18 h p.i., mRNAs were purified from the cells, and the viral mRNA levels were determined by reverse transcription-quantitative PCR as previously described (40). Data represent the means ± SD of results from triplicate samples. (B) Growth kinetics. Monolayers of Vero/hSLAM cells were infected with recombinant MVs (○, ICΔC-add[IC-C]; △, ICΔC-add[Ed-C]; ●, IC/EdPΔC-add[IC-C]; ▲, IC/EdPΔC-add[Ed-C]) at an MOI of 0.01. At various time intervals, the infectious virus titers were determined by plaque assays. Data represent the means ± SD of results from triplicate samples. (C) Plaque assays. Monolayers of Vero/hSLAM cells on 12-well cluster plates were infected with recombinant viruses and overlaid with Dulbecco modified Eagle medium containing 2% fetal bovine serum and 1% methylcellulose. At 6 days p.i., the cells were stained with the RTU Vectastain Elite ABC reagent (Vector Laboratories) using anti-MV H protein monoclonal antibodies and a biotinylated secondary antibody.

provide clues toward understanding why MV vaccine strains have become attenuated during the process of adaptation to growth in unnatural host cells and which viral proteins have contributed to this attenuation.

We thank M. A. Billeter for providing the p(+)MV2A plasmid encoding the genome of the Edmonston tag strain.

This work was supported by grants from the Ministry of Education, Culture, Sports, Science and Technology and the Ministry of Health, Labor and Welfare of Japan.

REFERENCES

1. **Andrejeva, J., K. S. Childs, D. F. Young, T. S. Carlos, N. Stock, S. Goodbourn, and R. E. Randall.** 2004. The V proteins of paramyxoviruses bind the IFN-inducible RNA helicase, mda-5, and inhibit its activation of the IFN-beta promoter. Proc. Natl. Acad. Sci. USA **101**:17264–17269.
2. **Bankamp, B., G. Hodge, M. B. McChesney, W. J. Bellini, and P. A. Rota.** 2008. Genetic changes that affect the virulence of measles virus in a rhesus macaque model. Virology **373**:39–50.
3. **Bankamp, B., J. Wilson, W. J. Bellini, and P. A. Rota.** 2005. Identification of naturally occurring amino acid variations that affect the ability of the measles virus C protein to regulate genome replication and transcription. Virology **336**:120–129.
4. **Baricevic, M., D. Forcic, T. K. Gulija, R. Jug, and R. Mazuran.** 2005. Determination of the coding and non-coding nucleotide sequences of genuine Edmonston-Zagreb master seed and current working seed lot. Vaccine **23**:1072–1078.
5. **Baron, M. D., A. C. Banyard, S. Parida, and T. Barrett.** 2005. The Plowright vaccine strain of Rinderpest virus has attenuating mutations in most genes. J. Gen. Virol. **86**:1093–1101.
6. **Baron, M. D., Y. Kamata, V. Barras, L. Goatley, and T. Barrett.** 1996. The genome sequence of the virulent Kabete "O" strain of rinderpest virus: comparison with the derived vaccine. J. Gen. Virol. **77**:3041–3046.
7. **Billeter, M. A., H. Y. Naim, and S. A. Udem.** 2009. Reverse genetics of measles virus and resulting multivalent recombinant vaccines: applications of recombinant measles viruses. Curr. Top. Microbiol. Immunol. **329**:129–162.
8. **Borges, M. B., E. Caride, A. V. Jabor, J. M. Malachias, M. S. Freire, A. Homma, and R. Galler.** 2008. Study of the genetic stability of measles virus CAM-70 vaccine strain after serial passages in chicken embryo fibroblasts primary cultures. Virus Genes **36**:35–44.
9. **Bryce, J., C. Boschi-Pinto, K. Shibuya, and R. E. Black.** 2005. W. H. O. estimates of the causes of death in children. Lancet **365**:1147–1152.
10. **Caignard, G., M. Guerbois, J. L. Labernardiere, Y. Jacob, L. M. Jones, F. Wild, F. Tangy, and P. O. Vidalain.** 2007. Measles virus V protein blocks Jak1-mediated phosphorylation of STAT1 to escape IFN-alpha/beta signaling. Virology **368**:351–362.
11. **Devaux, P., G. Hodge, M. B. McChesney, and R. Cattaneo.** 2008. Attenuation of V- or C-defective measles viruses: infection control by the inflammatory and interferon responses of rhesus monkeys. J. Virol. **82**:5359–5367.
12. **Devaux, P., V. von Messling, W. Songsungthong, C. Springfeld, and R. Cattaneo.** 2007. Tyrosine 110 in the measles virus phosphoprotein is required to block STAT1 phosphorylation. Virology **360**:72–83.
13. **Druelle, J., C. I. Sellin, D. Waku-Kouomou, B. Horvat, and F. T. Wild.** 2008. Wild type measles virus attenuation independent of type I IFN. Virol. J. **5**:22.
14. **Emeny, J. M., and M. J. Morgan.** 1979. Regulation of the interferon system: evidence that Vero cells have a genetic defect in interferon production. J. Gen. Virol. **43**:247–252.
15. **Escoffier, C., S. Manié, S. Vincent, C. P. Muller, M. Billeter, and D. Gerlier.** 1999. Nonstructural C protein is required for efficient measles virus replication in human peripheral blood cells. J. Virol. **73**:1695–1698.
16. **Fontana, J. M., B. Bankamp, W. J. Bellini, and P. A. Rota.** 2008. Regulation of interferon signaling by the C and V proteins from attenuated and wild-type strains of measles virus. Virology **374**:71–81.
17. **Griffin, D. E.** 2007. Measles virus, p. 1551–1585. *In* D. M. Knipe, P. M. Howley, D. E. Griffin, R. A. Lamb, M. A. Martin, B. Roizman, and S. E. Straus (ed.), Fields virology, 5th ed. Lippincott Williams & Wilkins, Philadelphia, PA.
18. **Hashimoto, K., N. Ono, H. Tatsuo, H. Minagawa, M. Takeda, K. Takeuchi, and Y. Yanagi.** 2002. SLAM (CD150)-independent measles virus entry as revealed by recombinant virus expressing green fluorescent protein. J. Virol. **76**:6743–6749.
19. **Kobune, F., H. Sakata, and A. Sugiura.** 1990. Marmoset lymphoblastoid cells as a sensitive host for isolation of measles virus. J. Virol. **64**:700–705.
20. **Longhi, S.** 2009. Nucleocapsid structure and function. Curr. Top. Microbiol. Immunol. **329**:103–128.
21. **Mosca, J. D., and P. M. Pitha.** 1986. Transcriptional and posttranscriptional regulation of exogenous human beta interferon gene in simian cells defective in interferon synthesis. Mol. Cell. Biol. **6**:2279–2283.
22. **Nakatsu, Y., M. Takeda, S. Ohno, R. Koga, and Y. Yanagi.** 2006. Translational inhibition and increased interferon induction in cells infected with C protein-deficient measles virus. J. Virol. **80**:11861–11867.
23. **Nakatsu, Y., M. Takeda, S. Ohno, Y. Shirogane, M. Iwasaki, and Y. Yanagi.** 2008. Measles virus circumvents the host interferon response by different actions of the C and V proteins. J. Virol. **82**:8296–8306.
24. **Nishie, T., K. Nagata, and K. Takeuchi.** 2007. The C protein of wild-type

measles virus has the ability to shuttle between the nucleus and the cytoplasm. Microbes Infect. 9:344–354.
25. **Ohno, S., N. Ono, M. Takeda, K. Takeuchi, and Y. Yanagi.** 2004. Dissection of measles virus V protein in relation to its ability to block alpha/beta interferon signal transduction. J. Gen. Virol. **85**:2991–2999.
26. **Palosaari, H., J.-P. Parisien, J. J. Rodriguez, C. M. Ulane, and C. M. Horvath.** 2003. STAT protein interference and suppression of cytokine signal transduction by measles virus V protein. J. Virol. **77**:7635–7644.
27. **Parks, C. L., R. A. Lerch, P. Walpita, H.-P. Wang, M. S. Sidhu, and S. A. Udem.** 2001. Comparison of predicted amino acid sequences of measles virus strains in the Edmonston vaccine lineage. J. Virol. **75**:910–920.
28. **Patterson, J. B., D. Thomas, H. Lewicki, M. A. Billeter, and M. B. Oldstone.** 2000. V and C proteins of measles virus function as virulence factors in vivo. Virology **267**:80–89.
29. **Radecke, F., and M. A. Billeter.** 1996. The nonstructural C protein is not essential for multiplication of Edmonston B strain measles virus in cultured cells. Virology **217**:418–421.
30. **Radecke, F., P. Spielhofer, H. Schneider, K. Kaelin, M. Huber, C. Dotsch, G. Christiansen, and M. A. Billeter.** 1995. Rescue of measles viruses from cloned DNA. EMBO J. **14**:5773–5784.
31. **Reutter, G. L., C. Cortese-Grogan, J. Wilson, and S. A. Moyer.** 2001. Mutations in the measles virus C protein that up regulate viral RNA synthesis. Virology **285**:100–109.
32. **Richardson, C. D., A. Scheid, and P. W. Choppin.** 1980. Specific inhibition of paramyxovirus and myxovirus replication by oligopeptides with amino acid sequences similar to those at the N-termini of the F1 or HA2 viral polypeptides. Virology **105**:205–222.
33. **Rivals, J. P., P. Plattet, C. Currat-Zweifel, A. Zurbriggen, and R. Wittek.** 2007. Adaptation of canine distemper virus to canine footpad keratinocytes modifies polymerase activity and fusogenicity through amino acid substitutions in the P/V/C and H proteins. Virology **359**:6–18.
34. **Rota, J. S., Z. D. Wang, P. A. Rota, and W. J. Bellini.** 1994. Comparison of sequences of the H, F, and N coding genes of measles virus vaccine strains. Virus Res. **31**:317–330.
35. **Schneider, H., K. Kaelin, and M. A. Billeter.** 1997. Recombinant measles viruses defective for RNA editing and V protein synthesis are viable in cultured cells. Virology **227**:314–322.
36. **Sekellick, M. J., W. J. Biggers, and P. I. Marcus.** 1990. Development of the interferon system. I. In chicken cells development in ovo continues on time in vitro. In Vitro Cell. Dev. Biol. **26**:997–1003.
37. **Shaffer, J. A., W. J. Bellini, and P. A. Rota.** 2003. The C protein of measles virus inhibits the type I interferon response. Virology **315**:389–397.
38. **Takeda, M., A. Kato, F. Kobune, H. Sakata, Y. Li, T. Shioda, Y. Sakai, M. Asakawa, and Y. Nagai.** 1998. Measles virus attenuation associated with transcriptional impediment and a few amino acid changes in the polymerase and accessory proteins. J. Virol. **72**:8690–8696.
39. **Takeda, M., S. Ohno, F. Seki, K. Hashimoto, N. Miyajima, K. Takeuchi, and Y. Yanagi.** 2005. Efficient rescue of measles virus from cloned cDNA using SLAM-expressing Chinese hamster ovary cells. Virus Res. **108**:161–165.
40. **Takeda, M., S. Ohno, M. Tahara, H. Takeuchi, Y. Shirogane, H. Ohmura, T. Nakamura, and Y. Yanagi.** 2008. Measles viruses possessing the polymerase protein genes of the Edmonston vaccine strain exhibit attenuated gene expression and growth in cultured cells and SLAM knock-in mice. J. Virol. **82**:11979–11984.
41. **Takeda, M., K. Takeuchi, N. Miyajima, F. Kobune, Y. Ami, N. Nagata, Y. Suzaki, Y. Nagai, and M. Tashiro.** 2000. Recovery of pathogenic measles virus from cloned cDNA. J. Virol. **74**:6643–6647.
42. **Takeuchi, K., S. I. Kadota, M. Takeda, N. Miyajima, and K. Nagata.** 2003. Measles virus V protein blocks interferon (IFN)-alpha/beta but not IFN-gamma signaling by inhibiting STAT1 and STAT2 phosphorylation. FEBS Lett. **545**:177–182.
43. **Takeuchi, K., N. Miyajima, F. Kobune, and M. Tashiro.** 2000. Comparative nucleotide sequence analysis of the entire genomes of B95a cell-isolated and Vero cell-isolated measles viruses from the same patient. Virus Genes **20**: 253–257.
44. **Takeuchi, K., M. Takeda, N. Miyajima, Y. Ami, N. Nagata, Y. Suzaki, J. Shahnewaz, S. Kadota, and K. Nagata.** 2005. Stringent requirement for the C protein of wild-type measles virus for growth both in vitro and in macaques. J. Virol. **79**:7838–7844.
45. **Tober, C., M. Seufert, H. Schneider, M. A. Billeter, I. C. D. Johnston, S. Niewiesk, V. ter Meulen, and S. Schneider-Schaulies.** 1998. Expression of measles virus V protein is associated with pathogenicity and control of viral RNA synthesis. J. Virol. **72**:8124–8132.
46. **Valsamakis, A., H. Schneider, P. G. Auwaerter, H. Kaneshima, M. A. Billeter, and D. E. Griffin.** 1998. Recombinant measles viruses with mutations in the C, V, or F gene have altered growth phenotypes in vivo. J. Virol. **72**:7754–7761.
47. **Yokota, S., H. Saito, T. Kubota, N. Yokosawa, K. Amano, and N. Fujii.** 2003. Measles virus suppresses interferon-alpha signaling pathway: suppression of Jak1 phosphorylation and association of viral accessory proteins, C and V, with interferon-alpha receptor complex. Virology **306**:135–146.

JOURNAL OF VIROLOGY, Jan. 2010, p. 372–379 Vol. 84, No. 1
0022-538X/10/$12.00 doi:10.1128/JVI.01690-09

Both RIG-I and MDA5 RNA Helicases Contribute to the Induction of Alpha/Beta Interferon in Measles Virus-Infected Human Cells[▽]

Satoshi Ikegame,[1,2] Makoto Takeda,[1]† Shinji Ohno,[1] Yuichiro Nakatsu,[1]†
Yoichi Nakanishi,[2] and Yusuke Yanagi[1]*

Department of Virology[1] and Research Institute for Diseases of the Chest,[2] Faculty of Medicine, Kyushu University, 3-1-1 Maidashi, Higashi-ku, Fukuoka 812-8582, Japan

Received 11 August 2009/Accepted 12 October 2009

Measles virus (MV), a member of the family *Paramyxoviridae*, is a nonsegmented negative-strand RNA virus. The RNA helicases retinoic acid-inducible gene I (RIG-I) and melanoma differentiation-associated gene 5 (MDA5) are differentially involved in the detection of cytoplasmic viral RNAs and induction of alpha/beta interferon (IFN-α/β). RIG-I is generally believed to play a major role in the recognition of paramyxoviruses, whereas many viruses of this family produce V proteins that can inhibit MDA5. To determine the individual roles of MDA5 and RIG-I in IFN induction after MV infection, small interfering RNA-mediated knockdown of MDA5 or RIG-I was performed in the human epithelial cell line H358, which is susceptible to wild-type MV isolates. The production of IFN-β mRNA in response to MV infection was greatly reduced in RIG-I knockdown clones compared to that in H358 cells, confirming the importance of RIG-I in the detection of MV. The IFN-β mRNA levels were also moderately reduced in MDA5 knockdown clones, even though these clones retained fully functional RIG-I. A V protein-deficient recombinant MV (MVΔV) induced higher amounts of IFN-β mRNA at the early stage of infection in H358 cells compared to the parental virus. The reductions in the IFN-β mRNA levels in RIG-I knockdown clones were less pronounced after infection with MVΔV than after infection with the parental virus. Taken together, the present results indicate that RIG-I and MDA5 both contribute to the recognition of MV and that the V protein promotes MV growth at least partly by inhibiting the MDA5-mediated IFN responses.

Alpha/beta interferons (IFN-α/β) play central roles in the host defense against viral infections (42). Pattern recognition receptors are the host molecules that detect pathogen-associated molecular patterns and activate the innate immune responses that operate at the early stage of infections (1). Toll-like receptor 3 (TLR3) and TLR7 recognize viral RNAs in the endosome and induce the production of various cytokines, including IFNs. In the cytoplasm of virus-infected cells, two RNA helicases, melanoma differentiation-associated gene 5 (MDA5) and retinoic acid-inducible gene I (RIG-I), are involved in virus recognition and IFN induction (21, 58, 59). Studies have shown that MDA5 recognizes long double-stranded RNAs (dsRNAs) (22), which are produced in cells infected with picornaviruses and reoviruses (23, 28), while RIG-I detects single-stranded RNAs with 5′-triphosphate (19, 37) and short dsRNAs (22), which are found in cells infected with a variety of RNA viruses. Therefore, it is generally believed that RIG-I plays a major role in the recognition of many RNA viruses, including paramyxoviruses (23, 28), whereas MDA5 only acts as an RNA sensor for certain RNA viruses.

Measles is a febrile acute infectious disease that remains a major cause of child deaths worldwide, especially in developing countries (7). Measles virus (MV) is a member of the genus *Morbillivirus* in the family *Paramyxoviridae*. The MV genome possesses six genes, which encode N (nucleocapsid), P (phospho-), M (matrix), F (fusion), H (hemagglutinin), and L (large) proteins, respectively (16). The P gene encodes two additional proteins, the V and C proteins (5, 10). During transcription of the P gene, an additional guanine residue may be inserted at a specific site in the nascent transcript via the recognition of an editing motif, producing the V mRNA (10). Consequently, the V protein shares the N-terminal 231 amino acid residues with the P protein but has a unique C-terminal region with 68 amino acid residues. The C protein is translated from the P and V mRNAs using an alternative reading frame (5). Although the V and C proteins are dispensable for MV growth in some cultured cells (40, 45), they promote viral replication by circumventing the host innate immune responses (11, 31, 53) and are associated with MV virulence in vivo (12, 35, 53, 54). The V protein blocks signal transduction in response to IFN-α/β (8, 13, 14, 32, 34, 41, 51, 57) and inhibits TLR7- and TLR9-mediated IFN-α/β production in human plasmacytoid dendritic cells by binding to IκB kinase α and IFN regulatory factor (IRF) 7 (36). Furthermore, the V proteins of many paramyxoviruses, including MV, bind to MDA5 and inhibit its function (2). Therefore, the role of MDA5 in the recognition of paramyxoviruses may have been underestimated in previous studies.

In the present study, we generated RIG-I and MDA5 knockdown human cells and a V protein-deficient recombinant MV (MVΔV) and examined the roles of RIG-I and MDA5 in the detection of MV and the resulting IFN induction. Our results indicated that these antiviral RNA helicase proteins both con-

* Corresponding author. Mailing address: Department of Virology, Faculty of Medicine, Kyushu University, 3-1-1 Maidashi, Higashi-ku, Fukuoka 812-8582, Japan. Phone: 81-92-642-6135. Fax: 81-92-642-6140. E-mail: yyanagi@virology.med.kyushu-u.ac.jp.
† Present address: National Institute of Infectious Diseases, Musashi-murayama, Tokyo 208-0011, Japan.
▽ Published ahead of print on 21 October 2009.

tribute to IFN induction in response to MV infection and that the V protein promotes MV growth at least partly by inhibiting the MDA5-mediated response in infected cells.

MATERIALS AND METHODS

Plasmid constructions. Using the pBAsi-hU6 pur DNA vector (Takara Bio, Inc., Shiga, Japan), we constructed three plasmids—pBAsi-MDA5, pBAsi-RIG-I, and pBAsi-luciferase—that generated stem-loop type small interfering RNAs (siRNAs). The siRNAs from pBAsi-MDA5, pBAsi-RIG-I, and pBAsi-luciferase targeted the mRNAs of human MDA5 and RIG-I and firefly luciferase, respectively. The target sequences for the human MDA5 and RIG-I and firefly luciferase mRNAs were 5′-GGAGAAUAACUCAUCAGAAUC-3′, 5′-GCCAGAAUCUUAGUGAGAAUU-3′, and 5′-GCCCGCGAACGACAUUUAUAA-3′, respectively.

The plasmid p(+)MV323-EGFP was derived from p(+)MV323, which encoded the full-length antigenomic cDNA of the virulent IC-B strain of MV, and contained an additional transcriptional unit for enhanced green fluorescent protein (EGFP) (17, 50). The plasmid p(+)MVΔV-EGFP was generated by introducing four nucleotide substitutions into the region corresponding to the RNA editing motif of the P gene of p(+)MV323-EGFP. All four substitutions were synonymous in the reading frame of the P protein. Recombinant MVs generated from p(+)MV323-EGFP and p(+)MVΔV-EGFP were designated wild-type (wt) MV and MVΔV, respectively, in the present study.

Cells and viruses. H358 (49), VV5-4 (3), and B95a (24) cells were maintained in RPMI 1640 medium (ICN Biomedicals, Aurora, OH) supplemented with 7.5% fetal bovine serum (FBS). To generate cells constitutively expressing the siRNAs targeting the mRNAs of human MDA5 and RIG-I and firefly luciferase, H358 cells cultured in 3.5-cm dishes were transfected with 5 μg of pBAsi-MDA5, pBAsi-RIG-I, or pBAsi-luciferase using Lipofectamine 2000 (Invitrogen Life Technologies, Carlsbad, CA), according to the manufacturer's instructions. At 36 h posttransfection, the cells were harvested, transferred onto 10-cm dishes, and selected in RPMI 1640 medium supplemented with 7.5% FBS and 1 μg of puromycin/ml. After 3 weeks of culture, the puromycin-resistant clones formed colonies on the 10-cm dishes, and three clones each were isolated from the pBAsi-MDA5-transfected cells (clones M1, M2, and M3) and pBAsi-RIG-I-transfected cells (clones R1, R2, and R3). One clone was also isolated from the pBAsi-luciferase-transfected cells. These clones were propagated for further analyses. Vero cells constitutively expressing human signaling lymphocyte activation molecule (SLAM) (Vero/hSLAM) (33) were maintained in Dulbecco's modified Eagle medium (ICN Biomedicals) supplemented with 7.5% FBS and 500 μg of Geneticin (G418; Nacalai Tesque, Tokyo, Japan)/ml. Recombinant MVs were generated in VV5-4 cells from the cloned cDNAs and propagated as described previously (29, 47).

Reagents and antibodies. A fusion blocking peptide (FBP), Z-D-Phe-Phe-Gly, was purchased from Peptide Institute (Osaka, Japan) (43). IFN-αA/D was purchased from Sigma-Aldrich (St. Louis, MO). A serum sample from a patient with subacute sclerosing panencephalitis (56) was kindly provided by M. B. A. Oldstone, The Scripps Research Institute, La Jolla, CA, and used to detect the MV N protein. Rabbit polyclonal antibodies against the MV P and V proteins and a mouse monoclonal antibody against the MV C protein (clone 2D10) were described previously (30, 31). Rabbit polyclonal antibodies against MDA5 and RIG-I were purchased from ProSci., Inc. (Poway, CA). A rabbit polyclonal antibody against IRF3 was purchased from Santa Cruz Biotechnology (Santa Cruz, CA). A mouse monoclonal antibody against human actin (clone C2) and a polyclonal antibody against IFN-induced protein with tetratricopeptide repeats 1 (ISG56) were purchased from Santa Cruz Biotechnology and Abnova Corp. (Taipei City, Taiwan), respectively. Horseradish peroxidase-conjugated donkey anti-rabbit and sheep anti-mouse immunoglobulin antibodies were purchased from GE Healthcare (Piscataway, NJ). A horseradish peroxidase-conjugated goat anti-human immunoglobulin antibody was purchased from EY Laboratories (San Mateo, CA).

Virus titration. Monolayers of Vero/hSLAM cells on 12-well plates were incubated with serially diluted virus samples for 1 h at 37°C, washed with phosphate-buffered saline, and overlaid with Dulbecco's modified Eagle medium containing 2% FBS and 1.5% methylcellulose 4000 (Wako Pure Chemical Industries, Osaka, Japan). At 5 days after infection, the numbers of PFU were determined.

Western blot analysis. After being washed with phosphate-buffered saline, cells were lysed with a buffer (150 mM NaCl, 10 mM Tris-HCl [pH 7.4], 1% Triton X-100, 1% sodium deoxycholate, 0.1% sodium dodecyl sulfate [SDS]), and the polypeptides in the lysates were reduced by heating in the presence of β-mercaptoethanol (Nacalai Tesque). For the detection of IRF3 dimers, cells were lysed with a different lysis buffer (150 mM NaCl, 50 mM Tris-HCl [pH 8.0], 1% NP-40) (20) supplemented with serine/threonine phosphatase inhibitor (Sigma-Aldrich), tyrosine phosphatase inhibitor (Sigma-Aldrich), and protease inhibitor cocktails (Sigma-Aldrich), and the polypeptides in the lysates were not reduced. The polypeptides were separated by SDS-polyacrylamide gel electrophoresis (PAGE), except for those prepared to detect IRF3 dimers, which were separated by native PAGE (20). The separated polypeptides were electroblotted onto polyvinylidene difluoride (PVDF) membranes (Hybond-P; GE Healthcare). The PVDF membranes were incubated with appropriate primary antibodies for 16 h at 4°C, washed three times with Tris-buffered saline containing 0.05% Tween 20 (TBST), and incubated with horseradish peroxidase-conjugated secondary antibodies for 1 h at room temperature. After three washes with TBST, the PVDF membranes were treated with ECL Plus reagents (GE Healthcare), and chemiluminescent signals were detected and visualized using a VersaDoc 3000 Imager (Bio-Rad, Hercules, CA). The relative amounts of the proteins were determined by densitometry using the Quantity One software (Bio-Rad).

Reverse transcription-quantitative PCR (RT-qPCR). Total RNAs were extracted and purified from cells using TRIzol reagent (Invitrogen Life Technologies), treated with RQ1 DNase (Promega, Madison, WI), and reverse transcribed into cDNAs by using a PrimeScript RT reagent kit and an oligo(dT) primer (Takara Bio, Inc.), according to the manufacturer's instructions. The amounts of cDNAs for the viral mRNAs and host β-actin and IFN-β mRNAs were quantified by using SYBR Premix Ex *Taq* II (Takara Bio, Inc.) and a LightCycler (Roche Diagnostics, Indianapolis, IN) as described previously (31, 48).

Transfection with MV leader RNA. MV leader RNA was synthesized in vitro by using a MEGAshortscript kit (Ambion, Austin, TX) according to the manufacturer's instructions, and the in vitro transcription products were purified by using TRIzol reagent as previously described (31). Monolayers of cells on six-well plates were transfected with 1 μg of MV leader RNA by using Lipofectamine 2000. Cellular RNAs were collected at 6 h posttransfection.

RESULTS

Generation of MDA5 or RIG-I knockdown cells. For the present study, we used the human epithelial cell line H358, which is susceptible to clinical MV isolates via an as-yet-unidentified receptor (49). Our preliminary results indicated that the V protein may play an important role in MV growth in H358 cells, since MV lacking the V protein exhibited reduced growth in this cell line, but not in other cell lines (see below). To evaluate the individual contributions of MDA5 and RIG-I to the induction of IFN-α/β after MV infection, we produced H358 cells that constitutively expressed siRNAs targeting the MDA5 and RIG-I mRNAs. Three MDA5 knockdown clones and three RIG-I knockdown clones were selected to minimize the effects of clonal variations. The expression levels of MDA5 and RIG-I were examined by Western blot analysis in these clones at 24 h after treatment with IFN-αA/D (Fig. 1), since MDA5 and RIG-I were only expressed at low levels without IFN treatment. The signal intensities for MDA5 and RIG-I were quantified and normalized by that for β-actin. All three MDA5 knockdown clones (M1, M2, and M3) expressed MDA5 at levels of <5% compared to the parental H358 cells, whereas the RIG-I knockdown clones (R1, R2, and R3) expressed RIG-I at levels of 5 to 35% compared to the parental H358 cells.

IFN-β mRNA expression in MDA5 and RIG-I knockdown clones after MV infection. IFN-β mRNA expression was examined by RT-qPCR in the MDA5 and RIG-I knockdown clones, as well as in H358 cells after infection with wt MV. A clone expressing a nontargeting luciferase siRNA was also included as a control for the analysis. The IFN-β mRNA levels were very low in all cells at 24 h after infection (data not shown). At 48 h after infection, all three RIG-I knockdown

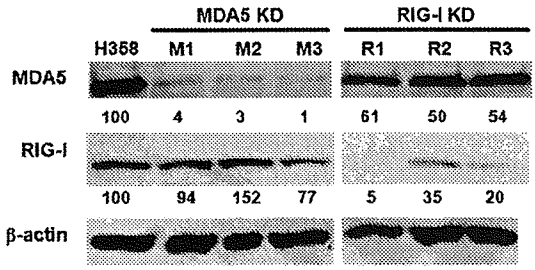

FIG. 1. Expression of MDA5 and RIG-I in H358 cells and knockdown clones. The expression levels of MDA5 and RIG-I in the parental H358 cells, MDA5 knockdown clones (MDA5 KD: M1, M2, and M3), and RIG-I knockdown clones (RIG-I KD: R1, R2, and R3) were examined by Western blot analysis at 24 h after treatment with IFN-αA/D. β-actin was evaluated as an internal control. Indicated blow each band are the signal intensities of MDA5 and RIG-I, which were normalized by that of β-actin. The value of the parental H358 cells was set to 100%.

clones produced IFN-β mRNA at levels of <5% compared to the parental H358 cells (Fig. 2A), in agreement with previous findings that RIG-I is a chief cytoplasmic RNA sensor for the detection of paramyxovirus infections (23, 28). H358 cells inoculated with wt MV in the presence of the FBP or with UV-inactivated wt MV expressed as low levels of IFN-β mRNA as the mock-infected cells, confirming that MV replication in the cytoplasm was required for the induction of IFN-β mRNA expression in H358 cells. Furthermore, the control H358 cells expressing a nontargeting siRNA produced almost the same amount of IFN-β mRNA as the parental H358 cells after infection with wt MV, indicating that the presence of siRNA per se does not affect the expression of IFN-β mRNA.

If RIG-I is largely responsible for detecting MV RNA, knockdown of MDA5 should not affect the expression levels of IFN-β mRNA in H358 cells. However, expression of IFN-β mRNA was reduced by 60 to 80% in the three MDA5 knockdown clones (Fig. 2A). To confirm that RIG-I was functioning properly in these MDA5 knockdown clones, the clones were treated with MV leader RNA transcribed in vitro, which has been shown to induce IFN-α/β via RIG-I (38). All three MDA5 knockdown clones, as well as the control clone expressing a nontargeting siRNA, expressed similar or even higher levels of IFN-β mRNA in response to the MV leader RNA compared to the parental H358 cells (Fig. 2B). As expected, the RIG-I knockdown clones exhibited reduced expression of IFN-β mRNA in response to the MV leader RNA. These results indicate that not only RIG-I but also MDA5 is involved in IFN induction after MV infection.

Generation and properties of a recombinant MV lacking the V protein. Many previous studies may have failed to demonstrate the contribution of MDA5 to IFN induction because paramyxoviruses produce V proteins that bind to MDA5, thereby inhibiting its function. To examine the activity of MDA5 in the absence of the V protein, we generated a recombinant MV incapable of producing the V protein (MVΔV). To this end, four point mutations were introduced into the P gene editing motif of wt MV, such that they were synonymous in the reading frame of the P protein (Fig. 3A). MVΔV grew efficiently in SLAM-positive B95a cells (data not

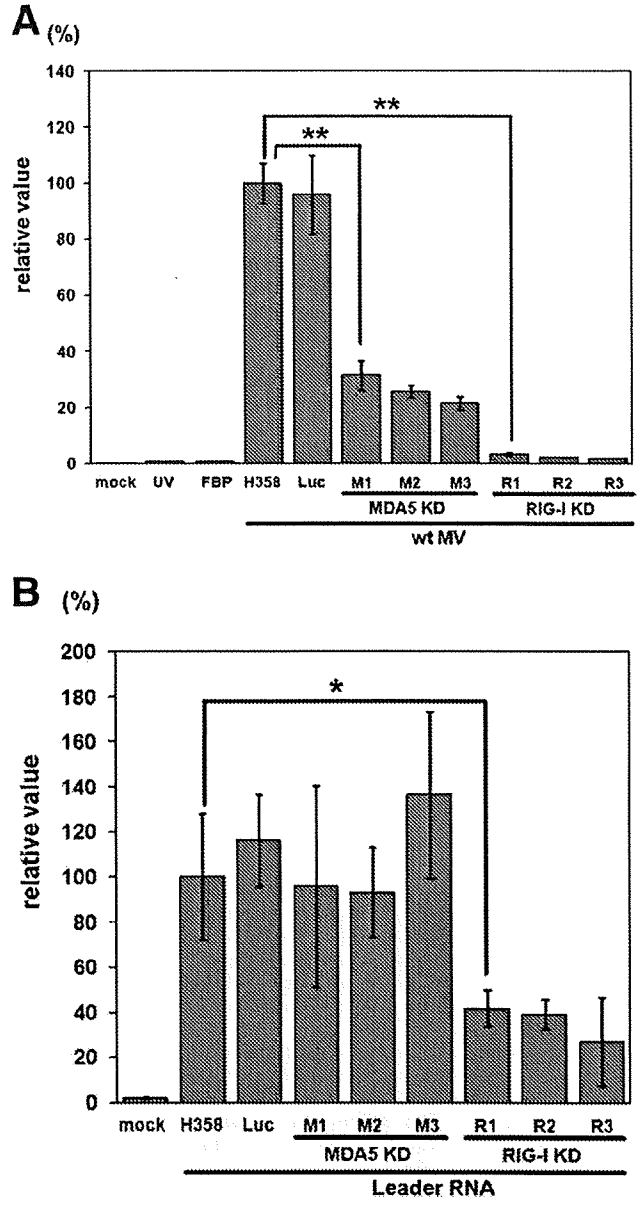

FIG. 2. IFN-β mRNA expression in H358 cells and knockdown clones after MV infection or transfection with MV leader RNA. (A) The parental H358 cells, the clone expressing a nontargeting luciferase siRNA (Luc), MDA5 knockdown clones (MDA5 KD: M1, M2 and M3) and RIG-I knockdown clones (RIG-I KD: R1, R2 and R3) were infected with wt MV at a multiplicity of infection (MOI) of 0.5. H358 cells were also infected with UV-inactivated wt MV (UV), treated with an FBP before wt MV infection (FBP), or mock infected (mock). Total RNAs were extracted from the cells at 48 h after infection, and the IFN-β mRNA levels were quantified by RT-qPCR. (B) H358 cells, the clone expressing a luciferase siRNA, and MDA5 and RIG-I knockdown clones were transfected with in vitro-transcribed MV leader RNA. H358 cells were also mock transfected (mock). Total RNAs were extracted from the cells at 6 h posttransfection, and the IFN-β mRNA levels were quantified by RT-qPCR. All data were normalized by the corresponding β-actin mRNA levels in the respective cells. The mean value in the parental H358 cells infected with wt MV (A) or transfected with MV leader RNA (B) was set to 100%. The data represent the means ± the standard deviations of triplicate samples. *, $P < 0.05$; **, $P < 0.01$ (significant differences based on a t test).

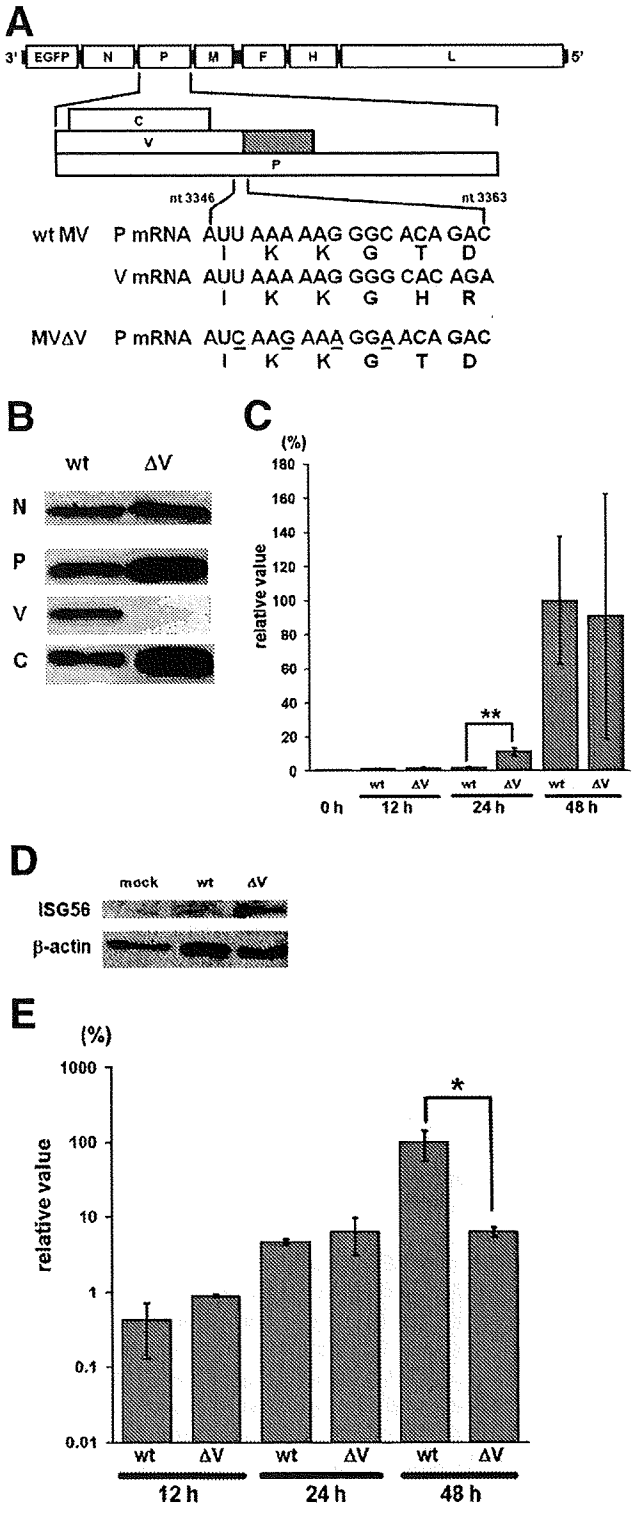

FIG. 3. Generation and properties of the V protein-deficient MV (MVΔV). (A) Diagram of the MV genome indicating the locations of the introduced mutations to generate MVΔV. Underlines indicate the mutated nucleotides. The predicted amino acids are shown below the trinucleotide codons. nt, nucleotide. (B) Protein synthesis in MV-infected cells. B95a cells were infected with wt MV or MVΔV at an MOI of 0.01. At 36 h after infection, viral proteins (N, P, V, and C) in the infected cells were detected by Western blot analysis. (C) IFN-β mRNA levels in H358 cells infected with wt MV or MVΔV at an MOI of 0.5. At 12, 24, and 48 h after infection, total RNA was extracted from the MV-infected cells, and the IFN-β mRNA levels were quantified by RT-qPCR. The data were normalized by the β-actin mRNA levels, and the mean value in wt MV-infected cells at 48 h after infection was set to 100%. The data represent the means ± the standard deviations of triplicate samples. The IFN-β mRNA level in uninfected cells is also shown (0 h). **, $P < 0.01$ (significant difference based on a t test). (D) Induction of ISG56 in MV-infected cells. H358 cells were mock infected or infected with wt MV or MVΔV at an MOI of 0.5. At 24 h after infection, the ISG56 levels in the infected cells were detected by Western blot analysis. β-Actin was analyzed as an internal control. (E) N mRNA levels in H358 cells infected with wt MV or MVΔV at an MOI of 0.5. At 12, 24, and 48 h after infection, total RNA was extracted from MV-infected cells, and the N mRNA levels were quantified by RT-qPCR. The data were normalized by the β-actin mRNA levels, and the mean value in wt MV-infected cells at 48 h after infection was set to 100%. *, $P < 0.05$ (significant difference based on a t test).

shown). cDNAs of the P and V mRNAs from MVΔV-infected B95a cells were amplified by PCR, and the PCR products were cloned and sequenced to determine the frequency of the RNA editing. Although 42% (20/48) of the PCR products from wt MV-infected cells had one or more additional guanine residues at the editing site, none (0/45) of the PCR products from MVΔV-infected cells had any additional nucleotides. Western blot analysis further confirmed that the P and C proteins, but not the V protein, were produced in MVΔV-infected B95a cells (Fig. 3B).

In H358 cells, IFN-β mRNA production was hardly increased above the background (uninfected) level at 12 and 24 h after infection with wt MV (Fig. 3C). MVΔV induced ~6 times more IFN-β mRNA in H358 cells at 24 h after infection compared to wt MV. Similarly, MVΔV induced a larger amount of the IRF3-activated protein ISG56 at 24 h after infection compared to wt MV (Fig. 3D). At 12 and 24 h after infection, the amounts of the N mRNA determined by RT-qPCR were comparable between wt MV- and MVΔV-infected H358 cells (Fig. 3E). Therefore, a difference in the amounts of viral RNAs produced was unlikely to be responsible for the difference in the amounts of IFN-β mRNA and ISG56 induced. Taken together, these results suggest that the absence of the V protein led to enhanced activity of MDA5 in MVΔV-infected cells, which in turn caused higher inductions of IFN-β and ISG56. The amount of the N mRNA at 48 h after MVΔV infection was ~10-fold lower than that after wt MV infection (Fig. 3E), which was probably due to the higher levels of IFN induced at the early stage of infection (24 h after infection) in MVΔV-infected cells, resulting in the inhibition of virus replication. This reduction of MV replication (and therefore viral RNA synthesis) at later times in MVΔV-infected cells may also explain why at 48 h after infection, there is little difference in the amount of IFN produced between wt MV- and MVΔV-infected cells (Fig. 3C).

Infection of MDA5 and RIG-I knockdown cells with MVΔV. Next, we infected MDA5 and RIG-I knockdown clones, as well as H358 cells, with MVΔV. Detection of MV infection appeared to be suppressed in MVΔV-infected MDA5 knockdown clones, as evidenced by decreases in the production of